YUCATAN ANCHIALINE CAVES

LATE HOLOCENE (3500 yBP) SALINITY CHANGES AND THEIR CLIMATIC IMPLICATIONS AS RECORDED IN AN ANCHIALINE CAVE SYSTEM, OX BEL HA, YUCATAN, MEXICO

Jeremy Gabriel

A thesis

Submitted to the School of Geography and Earth Sciences

in partial fulfillment of the degree

Master of Science

Master of Science
(Geology)

McMaster University

TITLE: Late Holocene (3500 yBP) salinity changes and their climatic implications as recorded in an anchialine cave system, Ox Bel Ha, Yucatan, Mexico

AUTHOR: Jeremy J. Gabriel

SUPERVISOR: Dr. Eduard G. Reinhardt

NUMBER OF PAGES: vii, 103

ABSTRACT

Foraminifera and thecamoebians have been used extensively in coastal reconstructions and intertidal zonations. Recent work has shown that their distributions in anchialine cave systems are effective at characterizing modern hydrologic conditions and reconstructing climatic fluctuations over the mid-late Holocene. This thesis focuses on the lower extent (within 2 km of the Caribbean coast) of the Ox Bel Ha cave system in Tulum, Quintana Roo, Mexico.

Surface sediment samples and sediment push cores were collected along a shore-normal transect using SCUBA techniques. The samples were analyzed for foraminifera and thecamoebian populations to establish: (1) Their modern distributions in different locales in the cave system including open water cenotes, main cave passages, and secondary cave passages; and (2) Their transitions through the late Holocene (3500 yBP) in response to climatic fluctuations, particularly precipitation. Hydrochemical parameters (specific conductivity, luminescent dissolved oxygen, pH, and temperature) of the modern water column were obtained to complement the microfossil assemblages in the surface samples. The sediment push cores were age-constrained using radiocarbon techniques and organic matter geochemistry ($\delta^{13}C$, $\delta^{15}N$, TOC, TN, C/N) was used to determine the dominant source of sediment input.

Salinity is the main controlling factor on the presence of foraminifera and thecamoebians; however the sedimentation patterns in the cave system had a significant role in sample biasing. In the open water and main cave conduit,

sedimentation rates were higher (~0.22mm yr^{-1}) and the microfossil assemblage showed high abundances of *Ammonia tepida* and *Elphidium gunteri*, with a minor component being comprised of brackish thecamoebians *Centropyxis aculeata* and *C. constricta*. In the deeper areas of the cave where sedimentation rates were considerably lower the samples contained a more heterogeneous mix of *A. tepida, E. gunteri, C. aculeata,* and *C. constricta*. This biasing is important to consider when interpreting the core data.

The core records showed four distinct phases of climatic changes which are closely tied to fluctuations in precipitation over the late Holocene. Periods of increased precipitation resulted in higher turbulent mixing at the interface between the superior fresh meteoric water and the basal saline marine water (halocline), resulting in more brackish conditions in the groundwater overall. Alternatively, lower precipitation resulted in a freshening of the groundwater due to the decreased turbulent mixing at the halocline. In addition, periods with high fluctuations in precipitation caused a heterogeneous mix of microfossils as a result of poor time averaging due to the low sedimentation rates. This inverse relationship has important implications in understanding the different periods of the ancient Maya culture, particularly the transition between the Classic and Post-Classic Periods.

ACKNOWLEDGEMENTS

Firstly, I thank my supervisor Eduard Reinhardt for all his support and encouragement and for giving me the opportunity to work not only on this project, but others around the world. Also, for introducing me to the DIR method of SCUBA diving opening me up to a whole other world of diving, caves.

For helping with me laboratory and analytical procedures, I am grateful to the McMaster MicroPaleontology Lab: Pete van Hengstum, Jessica Pilarczyk, and Simon Donato. Also thanks go to Martin Knyf of the McMaster Stable Isotope Laboratory for analyzing the geochemistry of the organic and carbonate matter samples. For help understanding the complex hydrology of the Yucatan Peninsula and for collecting a lot of the hydrochemical profiles, I am thankful to Patricia A. Beddows.

I am thankful to Fred Devos, Daniel Riordan, and Christophe LeMaillot of Zero Gravity Dive Center, Mexico who taught me how to dive and provided invaluable assistance with cave maps and sample collection. Thanks also to the diving support of Blake Wilson and Eric Utigaard.

For everything else I am thankful to my family and friends for their ongoing support in all of my academics. I would not have made it this far without you.

TABLE OF CONTENTS

Chapter 1 - Introduction

Foraminifera and thecamoebians have been used extensively in coastal geology to define ecologic zonations within the intertidal systems (e.g. Charman et al., 2000; Barbosa et al., 2005; Berkeley et al., 2007, 2008), including mangroves (Barbosa, 2000). These zonations are very effective indicators of environmental changes such as sea-level rise (e.g. Patterson et al., 2005; Horton et al., 2007; Horton and Culver, 2008; Kemp et al., 2009), land-use disturbance (e.g. Culver and Buzas, 1995; Reinhardt et al., 2005), and organic matter input and nutrient loading (e.g. Escobar et al., 2008). However, their distribution in coastal anchialine cave systems is relatively unknown with only a few studies examining the variation in assemblages in this unique environment (Javaux and Scott, 2003; van Hengstum et al., 2008, 2009). Even fewer studies have attempted using them as indicators of palaeoenvironmental changes within the caves in response to rising sea level or climate change (Gabriel et al., 2009; van Hengstum et al., submitted).

The Yucatan Peninsula, Mexico is a large, low-lying carbonate platform comprised mostly of Eocene and younger limestone (Weidie, 1985) with a high primary porosity making it very susceptible to dissolution (Back et al., 1986) resulting in an expansive network of anastamosing cave systems. Quaternary sea-level fluctuations in the Caribbean Sea are the dominant factor controlling the formation of these caves as the mixing zone (halocline) between the fresh meteoric water and the saline marine water that make up the groundwater aquifer is a zone of increased dissolution as it is subsaturated with respect to carbonate (Hanshaw and Back, 1980; Back et al., 1986; Smart et al., 1988). The caves are accessible through collapsed sinkholes, locally known as cenotes, which form via several processes: (1) sub-aqueous dissolution of the cave ceiling by the subsaturated halocline; (2) sub-aerial dissolution by percolation of carbonic acid through the vadose zone; and (3) removal of the upward buoyant force of the groundwater as a result of sea-level drop (Smart et al., 1988; Schmitter-Soto et al., 2002). Due to the high primary porosity of the limestone (25 – 50%; Smart et al., 2006), meteoric water rapidly infiltrates the vadose zone and percolates down into the subterranean cave systems; the only access to the fresh water is through the cenotes. This would have made them a very important resource to the ancient Maya who occupied various regions of the Yucatan from ~2000 yBP until Spanish conquest in the 15th century (Sharer, 1994). It is believed that the control of fresh water resources allowed Maya kings to maintain power and that the loss of it resulted in the Classic Period collapse when many of the most prominent city centres were abandoned (e.g. Tikal, Calakmul, Caracol; Lucero, 2002; Johnston, 2004). The previous palaeoclimate research has been conducted on closed-system (i.e. no associated cave conduits), inland lakes (e.g. Curtis et al., 1996, 1998; Hodell et al. 2001, 2005). The data presented here exmines the changes to the groundwater aquifer of subterranean cave conduits that have open access to the Caribbean Sea.

This thesis uses core and surface sediment samples from the Ox Bel Ha cave system, located about 8.5 km south of Tulum, Quintana Roo, Mexico to: (1) characterize and document the species assemblage in the coastal anchialine cave and the relationship between hydrochemical parameters including dissolved oxygen (DO), pH, salinity and proximity to open water (cenotes); and (2) reconstruct late Holocene (< 3500 yBP) environmental changes in response to rising sea level and regional climate change through a multiproxy approach of microfossils and organic geochemistry (^{13}C and ^{15}N stable isotopes, total organic carbon and nitrogen, and the C/N ratio). In addition, it examines the relationship between environmental conditions in the cenote, namely salinity, and the occupation by the ancient Maya of the city of Tulum, which flourished between 950 cal yBP and 500 cal yBP.

The chapters of this thesis have been written in accordance with the styles of specific scientific journals. As such, some overlap may occur in the information presented in each chapter, particularly in the introduction and background research sections.

Chapter 2

Modern surface distributions of foraminifera and thecamoebians in a coastal anchialine cave system, Ox Bel Ha, Mexico, and their relation to sedimentation patterns.

Jeremy J. Gabriel, Eduard G. Reinhardt, Peter J. van Hengstum, and Patricia A. Beddows

This manuscript has been prepared for submission to Journal of Foraminiferal Research *and follows the formatting and referencing style of the journal.*

ABSTRACT

Surface sediment samples (n = 37) were collected from the lower reaches (up to 2 km from the coast) of the Ox Bel Ha cave system in Quintana Roo, Mexico. Hydrochemical characteristics (specific conductivity, luminescent dissolved oxygen, pH, and temperature) were measured using a Hydrolab CTD and recognized an upper water mass (0 – 10.5 m depth) with an average salinity of 5 – 6 ppt and LDO = 4.3 mg L^{-1}; the middle water mass (10.5 – 15 m depth) had an average salinity of 16 – 18 ppt and LDO between 0 and 0.1 mg L^{-1}; and the lower water mass (> 15 m) had a salinity of 33 ppt and LDO that ranged between 0 and 1.5 mg L^{-1}. LDO was likely controlled by the hydrologic flow in the cave passages. The main passages had a higher flow rate and higher LDO while the deeper secondary passages were virtually still resulting in very low LDO, especially at depth. Vertical salinity trends were due to the mixing of the upper freshwater with the underlying intrusive marine water.

Q-mode cluster analysis of the faunal distributions resulted in six assemblages associated with mid-range diversities (Shannon diversity index 1.5 – 2.2) and varied salinities. Assemblage 1 (mean 8.8 m, 6.7 ppt) is dominated by *Ammonia tepida* (57%). Assemblage 2 (mean 9.8 m, 11 ppt) is dominated by *Miliammina fusca* (42%) and lesser amounts of *Ammonia tepida* (20%). Assemblage 3 (mean 8.3 m, 5.7 ppt) was dominated by *Elphidium gunteri* (43%) and *Centropyxis constricta* (24%). Assemblages 1 through 3 were collected from the main cave passage that had higher sedimentation rates due to proximity to cenotes. Assemblage 4 (mean 16 m, 34 ppt) was dominated by *Physalidia simplex* (42%); only one sample made up this assemblage. Assemblage 5 (mean 12 m, 18 ppt) was dominated by *Ammonia tepida* (31%) and *Centropyxis constricta* "spinosa" (16%). Finally, assemblage 6 (mean 12 m, 13 ppt) was dominated by *Centropyxis constricta* "spinosa" (25%), *Centropyxis constricta* "aerophile" (13%), and *Ammonia tepida* (16%). Assemblages 4 through 6 were all located in the secondary cave passages where sedimentation rates were very lower due reduced hydrologic flows and isolation from sediment inputs (cenotes or karst windows). Due to these low sedimentation rates time averaging was very high in theses areas producing the mixed assemblages of thecamoebians and more marine taxa (eg. *Elphidium gunteri).*

INTRODUCTION

Anchialine cave systems are haline, subterranean aquifers with no surficial connection to open ocean and have restricted exposure to open air. These types of environments have been studied globally in neotropical (e.g. Iliffe, 1992; Smart and others, 2006), Indian Ocean (e.g. Namiotko and others, 2004), and circum-Pacific (e.g. Maddocks, 2005) karst coastlines where carbonate dissolution of limestone has formed extensive vadose and phreatic cave systems as a result of Quaternary sea-level oscillations (Smart and others, 1988; Mejia-Ortiz and others, 2007). On the Caribbean coast of the Yucatan Peninsula, Mexico, a large (300,000 km^2; Smart and others, 2006) low-lying carbonate platform, these caves are ubiquitous and are some of the longest in the world (QRSS, 2009). Recent advances in SCUBA (self-contained underwater breathing apparatus) techniques have allowed researchers to study the environmental conditions deep within the cave systems. The extreme conditions (e.g. no sunlight, low oxygen levels, fluctuating salinities) within these caves host a unique assemblage of macrofauna (crustaceans and fish) which share similar attributes to deep sea species (e.g. low pigmentation, lack of eyes; Iliffe, 1992). Researchers have also studied the bacteria, phytoplankton and other primary producers of the anchialine caves and cenotes (e.g. Sanchez and others, 2002; Schmitter-Soto and others, 2002), but microfauna such as foraminifera and thecamoebians are comparatively unknown. A few studies have documented their distribution (e.g. Javaux and Scott, 2003; van Hengstum et al. 2008, 2009), but these are still limited and a full understanding of ecological controls is not developed. This study documents foraminifera and thecamoebians from the lower reaches of the Ox Bel Ha cave system, near the town of Tulum on the Yucatan Peninsula (Fig. 1). Ox Bel Ha is currently the longest underwater cave system in the world with over 180 km of mapped cave passage and several cenotes of various sizes throughout the system. The objectives were to characterize and document the species assemblage in the coastal (0.5 – 2 km from the coast) anchialine cave and the relationship between environmental conditions including dissolved oxygen (DO), pH, salinity and proximity to open water (cenotes). This baseline information is important for interpreting palaeoenvironmental trends found in cave sediments (van Hengstum et al., submitted; Gabriel et al., submitted).

Regional Setting and Cave Physiography

The Yucatan Peninsula is mostly young (Eocene and younger), diagenetically immature reefal limestone with a thin, patchy cover of terra rosa soil (Beddows and others, 2007; Smart and others, 2006; Vacher and Mylroie, 2002; Weidie, 1985) and has been tectonically stable since the late Pleistocene (Szabo and others, 1978). Like many coastal karst systems, it contains a density stratified groundwater aquifer with meteoric fresh water sitting atop encroaching saline sea water (Fig. 2). The eastern coast of the Yucatan Peninsula receives a high annual rainfall (1000 – 1500 mm yr^{-1}) which quickly penetrates the highly permeable limestone and percolates through the vadose zone into subterranean conduits (Back and others, 1986). Due to its high primary porosity, the limestone of the Yucatan is very susceptible to dissolution, particularly at the mixing zone (halocline) between the saline sea water and fresh meteoric water, which is subsaturated with respect to carbonate (Smart and others, 1988; Hanshaw and Back, 1980). Factors such as climate change, coastal progradation and sea-level oscillations have changed the relative position and stratification of the halocline through time resulting in complex systems of anastomosing cave passages. Changes in sea level in the Caribbean basin will raise or lower the groundwater table accordingly. Coastal progradation, which has been occurring since sea level decelerated around 5000 years ago (Blanchon and others, 2002; Blanchon and Shaw, 1995), likely causing sediment build up along the coast impeding hydrologic discharge from the cave conduits (Vacher and Mylroie, 2002; Vacher and Wallis, 1992; Perry and others, 1989). As the discharge rates decrease and cave waters stabilize, stratification of the two water masses would become more defined (Beddows, 2001). Climate change has also likely affected this stratification with increased precipitation, such as during the Holocene Thermal Maximum (10.5 – 5.4 kya), where the halocline may have been depressed due increased mass of the meteoric water lens. As discussed in van Hengstum et al (submitted), the excess influx of meteoric water may have caused increased turbulence in the groundwater aquifer causing more mixing at the halocline and less stratification; however, this is the first study that has attempted to reconstruct palaeohydrological conditions in the cave environment and propose that this relationship may exist.

Access to the cave systems is through collapse sinkholes, locally known as cenotes (from the Yucatec Maya *dz'onot*, meaning "well"). There are no surficial rivers on the Yucatan due to the rapid percolation of meteoric water so the cenotes are the only source of fresh water and provide access to the groundwater aquifer. There are generally two types of cenotes: those formed by passage roof collapse, and pit cenotes. The former intersect with large (1 – 100 m wide) horizontal conduits which have a relatively significant hydrologic flow (1 – 12 cm s^{-1}), while pit cenotes do not intersect with horizontal conduits and thus their circulation is through the permeable limestone walls and much more limited (Beddows and others, 2007). Hydrologic flow rates in the meteoric water mass vary along a shore normal transect with velocities as high as 12 cm s^{-1} near the coast to less than 1 cm s^{-1} 10 km inland. The difference in velocity is for two reasons: (1) thinning of the fresh water lens results in higher flow to maintain constant discharge, and (2) water funnelling in to the large conduits from other secondary fractures at the coast increasing the volume of water (Moore and others, 1992).

The sources of sediment within the cave are abiotic precipitates (e.g. calcite rafts), erosion of limestone from the cave ceiling, microfossils (e.g. foraminifera, thecamoebians, diatoms) and organic matter. Calcite rafts form at the water surface of supersaturated waters (Taylor and Chafetz, 2004) so their presence in cave sediments potentially indicates a former water table. These rafts are transparent, euhedral crystals and are easily distinguished from the opaque, angular detrital limestone grains. Pohlman and others (1997) described three main sources of organic matter into the caves. The first is transport of algal detritus from the cenotes by groundwater flow, the second is percolation of forest soil through cracks and fissures in the limestone via meteoric water, and finally coastal-borne organic matter brought in through tidal exchange. The total organic carbon in the cave sediments is generally high near the cenotes and cave entrance (25 – 50%) and drops drastically moving into the cave (0.1 – 1.9%, > 60 m from the cave entrance; Pohlman and others, 1997).

Foraminifera and Testate Amoebae in Anchialine Caves

Significant coastal research has been conducted on foraminifera and thecamoebians and their distribution in intertidal environments has been well documented throughout the world (e.g. Berkeley and others, 2008; Horton and Culver, 2008; Berkeley and others, 2007; Barbosa, 2000). An important environment that is currently being studied is within low salinity regimes (0.5 – 5 psu), such as salt marshes, in order to characterize the transition from thecamoebian-dominated to foraminifera-dominated systems (e.g. Riveiros and others, 2007; Usera and others, 2004; Charman and others, 2002).

Coastal anchialine caves represent a unique low salinity environment that is starting to be explored more frequently as a result of advances in SCUBA technology, which allows divers to explore further and stay down longer in order to conduct thorough surveys. Javaux and Scott (2003) conducted a large scale investigation of several coastal environments in Bermuda including marine caves, landlocked ponds, lagoons, reefs, and mangrove swamps to document the foraminiferal assemblages. The caves contained an array of calcareous and agglutinated foraminifera including *Ammodiscus tenuis*, *Tiphotrocha comprimata*, *Rosalina* spp., *Elphidium* spp., *Triloculina oblonga*, and *Helenina anderseni*, though no data were presented regarding the low-salinity transitions between agglutinated and calcareous assemblages. van Hengstum and others (2008) presented the first systematic description of foraminifera and thecamoebian distributions within three anchialine cenotes on the Yucatan Peninsula and how they were related to environmental parameters including salinity and dissolved oxygen (DO). Surface samples from three different cenotes, with a salinity range between 1.5 and 3.3 ppt, showed a range of foraminifera and thecamoebian species. The lowest salinity (1.5 ppt; Aktun Ha) had assemblages dominated by *Centropyxis aculeata* "aculeata" and *Arcella vulgaris*, mid-range salinities (~3 ppt; Maya Blue) were comprised of *C. aculeata* "aculeata" and *C. aculeata* "discoides", and the higher salinities (> 3.4 ppt; El Eden) had high abundances of *Ammonia tepida*, *Jadammina macrescens*, *Tritaxis fusca*, and *C. constricta* "spinosa" and *C. constricta* "aerophile". A salinity of ~3.5 ppt was shown to be an important transition from thecamoebian-dominated to foraminifera-dominated assemblages, with *C. constricta* "aerophile" being the most euryhaline thecamoebian.

In the Aktun Ha cave system, van Hengstum and others (2009) surveyed the transition of foraminifera and thecamoebian populations from the fresh surface waters (1.5 ppt) down through the halocline into the basal marine water

(35 ppt). In addition to the thecamoebian species found in the other cenotes, they also discovered *Difflugia* spp. and *Lagenodifflugia vas* living in the shallow cave, though they were not seen in the open water cenotes. In the more saline waters, *Bolivina striatula* and *B. variabilis* were found to be the dominant taxa, with *Elphidium* sp. and *Rosalina subaracuana* also present.

Gabriel and others (2009) presented the first palaeoenvironmental reconstruction of a cenote (Aktun Ha) using a sediment core obtained from the top of the collapse pile. Microfossils were essentially absent from most of the core except for the top 7 cm, which contained a very large population of *Physalidia simplex* (identified as *A. tepida* var. "juvenile") that colonized the brackish cenote as it flooded due to Holocene sea-level rise. Subsequently, van Hengstum and others (submitted) analysed sediment cores collected in the shallow cave both upstream and downstream of Aktun Ha cenote. Their results show that higher salinity oligohaline regimes (3.5 – 5 ppt) host populations with high abundances of *Physalidia simplex* and other hyaline foraminifera including *A. tepida* and *B. striatula*. As salinity decreases, *Centropyxis* spp. start to increase in abundance (1.5 – 3.5 ppt) and finally the assemblages are dominated by lacustrine thecamoebians *Difflugia oblonga* and *Lagenodifflugia vas* (< 1.5 ppt). Once again, the transition from foraminifera-dominated assemblages to thecamoebian-dominated assemblages occurred around 3.5 ppt. These changes were related to changing inflows of rainwater over Holocene climatic cycles.

STUDY SITE

The Ox Bel Ha cave system is located on the Caribbean coast approximately 8.5 km south of the town of Tulum (Fig. 1). It is the longest underwater cave system in the world with 180 km of explored anastomosing cave passages that extend from the coast inland for more than 2.5 km. There are several cenotes along the system, although primary access is through cenote Yax Chen, which is a large diamond-shaped sinkhole (13,500 m^2) that is located within 300 m of the coast and 125 m of the road. The bottom of the cenote is covered with massive limestone blocks as a result of ceiling collapse and generally has a depth of around 7.5 m though deeper crevasses can be found between the rocks. The main cave conduit starts at the northwest corner of the cenote and runs southwest for approximately 425 m, before turning and trending northwest. The main cave passage has an average depth of 8.8 m though depths as great as 13 m can be found in some areas. There are ten cenotes of various sizes along the main cave line of the studied section. The secondary cave passages tend to be deeper, with an average of depth of 12.8 m in the "Connector Line" section, 14.1 m in Little Chen, and 17.1 m in Arizona. This cave system is still being actively explored so a complete map showing depths and conduit size is not available. This study surveyed the first 2.6 km of the main cave line including three secondary cave passages, known as the "Connector Line", Little Chen, and Arizona.

METHODS

Thirty-seven surface sediment samples (< 5 cm) were collected from cave passages along the main line (ML; *n* = 17), secondary cave passages (SC; *n* = 16), and the open water cenotes (OW; *n* = 4) using SCUBA techniques and underwater scooters (Diver Propulsion Vehicles; DPV) to allow deeper penetrations. Samples were collected between June 2007 and May 2008 (Fig. 3). Hydrochemical profiles (horizontal and vertical) were collected using a HydroLab MS5 submersible, multi-parameter probe to measure specific conductivity (accuracy ± 0.5% of reading + 0.001 mS/cm), pH (accuracy ± 0.2 units), luminescent dissolved oxygen (LDO; accuracy ± 0.2 mg L^{-1}), and temperature. The vertical water profiles were collected by the diver rising slowly to the top of the cave and then slowly descending while gently swimming forward to obtain undisturbed readings (Beddows and others, 2007). These vertical profiles provide a very accurate description of the hydrochemical changes through the water column.

The sediment samples were stored in a dark, cool refrigerator until they were ready for analysis. Sediment samples were rinsed over 250, 125, and 45 µm sieves in order to concentrate and retain thecamoebians and foraminifera and divided using a wet splitter (Scott and Hermelin, 1993). Between 200 and 300 specimens were counted in each sample using an Olympus binocular dissecting microscope (up to 80x). Thecamoebian taxonomy generally follows Medioli and Scott (1983) and tests were identified to the strain level (Reinhardt and others, 1998) while the foraminifer taxonomy follows Gabriel et al (2009) and van

Hengstum et al (2009; 2008). The total assemblage has been shown to better represent the environmental conditions at a given site (Scott and Medioli, 1980), so no distinction was made between the living and the dead assemblages in this study. Previous work by van Hengstum et al., (2009) showed the rose bengal staining produced statistically insignificant numbers for examining live versus dead tests. There were a total of four thecamoebian species and fourteen foraminifer species identified within the cave system (Plate 1, Table 1). The relative fractional abundance of each species was calculated, with respect to the total population of thecamoebians and foraminifera, such that

$$F_i = \frac{C_i}{N_i}$$

where C_i is the individual species count and N_i is the total population. Statistically significant species were determined by calculating each species' standard error using the formula

$$S_{F_i} = 1.96\sqrt{\frac{F_i(1-F_i)}{N_i}}$$

In any case where the standard error of a species was greater than its fractional abundance in all samples, that species was deemed statistically insignificant and excluded from the multi-variate analysis (Patterson and Fishbein, 1989).

The Shannon-Weaver Diversity Index (SDI) was used to determine the environmental stability of each sample. The SDI takes into account the fractional abundance of each species in a sample and the species richness of that sample to establish the relative diversity according to the equation

$$SDI = -\sum_{i=1}^{S} \frac{C_i}{N_i} * \ln\left(\frac{C_i}{N_i}\right)$$

where S is the total number of species in the sample (richness). Patterson and Kumar (2002) determined that an SDI > 2.5 indicated stable conditions, 1.5 – 2.5 were transitional conditions, and < 1.5 indicated stressed conditions. Although originally used for thecamoebian populations, they have subsequently been used in a salt marsh environment on thecamoebians and foraminifera collectively (Riveiros and others, 2007).

Q-mode cluster analysis was performed on all samples using the statistical freeware package *PAST* (Hammer and others, 2001). Ward's method of minimum variance was used to cluster individual samples which were compared using a simple Euclidean distance coefficient and presented in a hierarchical dendrogram. Samples S34 – S37, inclusive, were not included in the cluster analysis as these samples did not contain any statistically significant populations.

RESULTS

Water Chemistry

The hydrogeochemical profiles revealed three distinct water masses within the cave system that had significantly different salinities (Fig. 4). The three profiles were all collected at different times of the year. The uppermost water mass (UWM; 0 – 10.5 m) had a fairly consistent salinity around 5.7 ppt, LDO saturation of 91%, pH of 6.8, and temperature of 26°C. The first halocline (HC1) occurs at ~10.5 m and separates the UWM from the middle water mass (MWM;

~10.8 m to 15 m). Here the salinity drastically increases to approximately 18.5 ppt and the pH goes up to about 7.2, though temperature and LDO saturation stay fairly constant. Most of the ML passage only goes deep enough to intersect with the first halocline; only at S29 and S33 does it drop below a second halocline (HC2), which occurred at ~15 m. Below this halocline (Lower Water Mass; LWM) salinity increases to 35 ppt and the temperature increases to almost 27°C. The LWM was found in the Little Chen and Arizona sections of the cave. The vertical profiles taken from the SC areas Little Chen and Arizona show quite different hydrochemical characteristics. The vertical profiles from both of these areas intersect both haloclines at approximately the same depths; however the other parameters show different patterns. In Little Chen, the UWM has a DO saturation of around 12% which decreases drastically through HC1 (10.5 m) to about 1% and then remains constant down to 15 m. In Arizona, the opposite is seen with DO saturation close to 0% through the UWM and MWM with no significant change until HC2 (15 m) where it gradually rises, reaching 30% at ~20 m and then decreases to 20% by 22.5 m. The other major difference is in the pH. Little Chen has a pH of ~7 through the UWM and MWM and then a slight increase to 7.3 below HC2. Arizona has a higher initial pH of 7.25 in the UWM which drops significantly to 6.9 through the MWM and then returns to the previous conditions, ~7.3, in the LWM. While the pH in both systems does not change enough to affect the microfossil populations, the lack of DO in the MWM

– LWM in Little Chen and in the UWM – LWM in Arizona will have a significant effect (Murray, 2006).

Microfaunal Zonation

Out of the fourteen species of foraminifera that were counted, three of them (*Bolivina* spp., *Helenina anderseni*, and *Haplophragmoides wilberti*) were excluded from cluster analysis due to a higher standard error than fractional abundance in all samples, making them statistically insignificant; all of the thecamoebian species were considered significant.

The dendrogram produced by the Q-mode cluster analysis resulted in six ecological assemblages to be defined (Fig. 5, Table 2). Samples S34 – S37 were manually grouped together as the seventh assemblage based on the near absence of any microfossils; only a few *Ammonia tepida* and *Elphidium* spp. tests were observed. Two of the assemblages did not seem to correspond to any known variable based on the ecology of the taxa. The assemblages were plotted on a ternary diagram according to fractional abundance of thecamoebians, agglutinated foraminifera, and calcareous foraminifera to illustrate the trend from low salinity brackish to more saline waters (Fig. 6; van Hengstum et al., 2008). Assemblage 1 (A1) contains eleven samples, of which seven are found within the first 300 m of the cave (S2 – S8). The sample from within Tarpon I cenote is also part of this assemblage (S11), as are two samples from the Connector Line area (S19 and S23), and one from upstream of Gemini I cenote (S32). The average depth of all the samples in A1 is 8.8 m with a SDI of 1.44, indicating a transitional assemblage. The average salinity is 6.68 ppt with a standard deviation of 3.23. A1 is dominated by the euryhaline foraminifer *A.tepida* (mean 57%), with low abundances (<10%) of the other species. The thecamoebian species *Centropyxis aculeata* and *C. constricta* combine to make up 16.7% of this assemblage. The centropyxids were further subdivided into ecophenotypes based on the presence or absence of spines (Reinhardt and others, 1998). *C. aculeata* "aculeata" and *C. constricta* "spinosa" are characterized by the presence of spines on the aboral region—we have observed up to 18 spines on *C. aculeata* "aculeata" and up to 8 on *C. constricta* "constricta". *C. aculeata* "discoides" and *C. constricta* "aerophile" are both lacking spines on the aboral region. Some studies (e.g. van Hengstum and others, 2008; Riveiros and others, 2007; Gehrels and others, 2001) have shown a link between ecophenotypes and salinity with the species without spines (i.e. "discoides" and "aerophile") being more euryhaline and tolerant to higher salinities. In A1, both ecophenotypes are present in similar abundances (with spines, 10.3%; without spines, 6.4%). On the ternary diagram, A1 plots in the lower right area due to the dominance of *A. tepida* and the small abundances of agglutinated foraminifera and thecamoebians.

Assemblage 2 (A2) consists of four samples. Three of the samples are found within 100 m of a cenote or in close proximity to dissolution holes in the cave ceiling (S24); S26 is found further upstream and off in an SC. The average depth of A2 is still within the UWM, though close to the halocline (9.8 m) and the

SDI is 1.84, which although slightly higher than A1 is still classified as transitional. The dominant taxon in this sample is the agglutinated foraminifera *Miliammina fusca* (mean 41.9%), followed by *A. tepida* (mean 20.2%). *Centropyxis* spp. combine to make up 18% of the assemblage with the ecophenotypes with spines becoming more abundant than those without (12.2% and 5.8%, respectively). The average salinity for A2 is 9.8 ± 0.8 ppt. This assemblage plots in the lower left corner of the ternary diagram due to the higher abundance of *M. fusca*.

Only two samples make up assemblage 3 (A3). Both of these samples are associated with a major cenote with S30 being just in the downstream cavern of Luna (<20 m) and S31 within the Gemini II cenote. The average depth of A3 is 8.3 ± 2.2 m, with an average salinity of 5.66 ± 0.06 ppt. The SDI in A3 is also at 1.84. The dominant taxon in A3 is *Elphidium gunteri* (mean 42.7%) though there is an increase in the abundance of *Centropyxis*, with a combined average of 31.2%. This assemblage also has the highest concentration of *Arcella vulgaris* (mean 8%). Due to high abundances of both thecamoebians and foraminifera, A4 plots mid-way up the right side of the ternary diagram.

Assemblage 4 (A4) only has one sample in it, which is found deep in the Little Chen secondary passage. The sample was collected from 16.1 m which puts it in the LWM at a salinity of 33.77 ppt. This sample is dominated by the calcareous foraminifer *Physalidia simplex* (42.1%), followed by *A. tepida* (24.6%). There is still a significant population of centropyxids (total 22.8%), which are mainly *C. constricta* "spinosa" (15.8%), and a small proportion of the agglutinated foraminifer *Ammodiscus tenuis* (7%). This sample had the lowest total concentration (45 cc^{-1}) of species likely due to the extremely low LDO saturation, which is nearly zero.

There are eight samples that make up assemblage 5 (A5). Aside from S1, which is located within Yax Chen cenote, the rest of the samples are found in the cave passage a fair distance (>200 m) away from a cenote. The average depth is 12.0 ± 3.3 m, which is in the MWM, and the average salinity is 17.8 ppt. *Ammonia tepida* is the dominant taxon in this assemblage (mean 30.6%) though overall thecamoebians and foraminifera are present in near-equal abundances (mean 39.3% and 37.3%, respectively). This assemblage plots close to the centre of the ternary diagram due to an almost equal abundance of calcareous and agglutinated foraminifera, and thecamoebians.

The final assemblage, A6, contains seven samples that are found in and around L-Shape cenote and the "Connector Line"; S10 is downstream from Tarpon I cenote. The samples had a mean depth of 12.0 ± 2.9 m and average salinity of 13.3 ppt. This assemblage also had the highest diversity index, mean 2.16, of any assemblage, which indicates that it is the most stable. *Centropyxis constricta* "spinosa" is the dominant taxon in this assemblage (mean 25%) and thecamoebians in total make up 57.4%. The ecophenotypes with spines are dominant over those without with average abundances of 34.2% and 19.3%, respectively. *Ammonia tepida* is the next most abundant species, with a mean of 15.9%, and the rest of the species are present in abundances lower than 10%.

The remaining samples (S34 – S37) make up assemblage 7 (A7). These samples were all collected from deep within the Arizona section of the cave, approximately 700 m from the main cave line. The sediments in this area were comprised entirely of calcite (raft crystals and limestone detritus; see Taylor and Chafetz, 2004). The LDO saturation in the UWM and MWM in Arizona is nearly 0% and then it rapidly increases below HC2 to about 20%. None of these samples had statistically significant populations of microfossils, even though three of the four samples were collected from below HC2.

DISCUSSION

The Ox Bel Ha cave system is a very complicated anchialine environment due mainly to its proximity to the coast. Mixing of the fresh, meteoric water and the saline ground water near the coast (< 4 km inland) results in very brackish waters, even in the so-called "fresh-water lens", due to increased shear from differential movement of the fresh and saline water (Beddows and others, 2007). The main factors controlling the assemblages are: (1) salinity, and (2) the sedimentation rate. In the lower areas of the system (i.e. closer to the coast) the sedimentation rate was higher as there was a thick cover of sediment (>1 m) blanketing the bottom of the cave passage; the abundance and proximity of cenotes providing a source of organic sediment into the cave (Pohlman and others, 1997; van Hengstum and others, 2009). The deeper secondary areas of the cave (e.g. Little Chen and Arizona) are removed from the main cave passage and are far from cenotes and sediment sources. The only sedimentation that occurs in these areas is detrital limestone eroding from the cave ceiling or calcite precipitation (i.e. calcite rafting; Taylor and Chafetz, 2004). With the lower sedimentation rates, the assemblage would be expected to be more time-averaged collecting tests over several environmental cycles. Sedimentation rates in the lower reaches (i.e. in the area of A1) of the cave system (Gabriel et al., submitted) are approximately 50-100 yrs/cm so lower sedimentation areas off the main cave passage the time averaging would be expected to be higher. Samples were collected from approximately the upper 2 cm so these assemblages could represent a time averaged assemblage of several hundred years. Similarly, in a deep area of Aktun Ha known as the Crystal Palace foraminifera collected on the surface were dated to Marine Isotope Stage 5e (124 – 119 kya; van Hengstum and others, 2009). These specimens were pristine (i.e. showed no taphonomic alteration) and were collected from beneath a piece of vadose flowstone eliminating the possibility of transport or erosion from the cave ceiling. Although this is likely an extreme case similar issues are a factor in the Ox Bel Ha surface samples.

Climate variability then acted with the low sedimentation rates to produce the mixed assemblage. Haug et al., (2001) showed climate variations (wet versus dry periods) from the Cariaco basin occurring quickly (less than 50 yrs) and Lake Chichancanab (Hodell and others, 2001), record precipitation fluctuations of approximately 50 years. These rapid climate fluctuations and the very low sedimentation rates (1cm = > 50 yrs; Gabriel et al., submitted) and variability throughout the system likely explains the differential mixture of thecamoebians and foraminifera in the samples (eg. thecamoebians mixed with the more marine taxa like *A. tepida* and *E. gunteri)* and the lack of correspondence with modern salinity conditions.

The hydrochemical characteristics of the water column could also factor in to the microfossil assemblages. The pH of the water varies throughout the cave system between ~6.7 and 7.3 ppt. The lower pH would cause higher dissolution of carbonate matter in the surface sediments, possibly affecting the abundance of calcareous foraminiferal species and agglutinated species that did not have an organic wall. Dissolved oxygen is another hydrochemical parameter that will have a significant effect on the microfossil populations. Some of the deeper areas of the cave system (below the halocline) have DO values close to zero. Foraminifera and thecamoebians require DO values of at least 1 mg L^{-1} to survive (Murray, 2006). A4 is located in a section of Little Chen where the DO is extremely low (<1 mg L^{-1} below 15 m), which has resulted in it having the lowest total concentration (45 cc^{-1}). Once again the presence of microfossils is the result of a greater time period influencing the sample and indicates that the DO has been above 1 mg L^{-1} in the past for these species to colonize this area of the cave. The modern salinity of the UWM averages between 5 and 6 ppt, which is outside the tolerance of centropyxids (< 3.5 ppt; van Hengstum and others, 2008) and therefore their presence would indicate biasing to the sample. Salinity shifts of only about 3 ppt are not uncommon in the UWM of the caves, particularly near the coast (Beddows and others, 2007). The shallow samples (i.e. those collected from the UWM) were generally collected from areas with higher sedimentation rates and typically have high abundances of agglutinated (mean 10%) and calcareous foraminifera (mean 66%) so these are likely indicative of a more contemporary assemblage (i.e. the taphocoenosis more closely resembles the biocoenosis). Approaching the halocline and moving into the MWM, the total abundance of thecamoebians in the samples starts to increase. These samples are typically located in the deeper secondary cave passages where the sedimentation rate is significantly lower and therefore they represent a longer time period and more environmental change (i.e. the taphocoenosis represents a higher proportion of the sample than the biocoenosis). This is also evident in the diversity indices. A5 and A6 had the greatest average depths (12.0 m) and the highest diversity indices (2.06 and 2.16, respectively). A sample that is an average of a greater time period and more environmental change will statistically appear more stable than one that is only representing a few fluctuations.

CONCLUSIONS

The dominant controlling factor on microfossil assemblages is salinity, with thecamoebians generally restricted to fresh water salinities < 3.5 ppt and foraminifera occupying the marine environment (van Hengstum and others, 2008). In most aquatic environments, such as exposed coastlines or inland lakes, there is a clear microfossil assemblage comprised of either foraminifera or thecamoebians, respectively (e.g. Barbosa, 2000; Charman and others, 2002; Riveiros and others, 2007). However, in oligohaline environments, such as salt marshes, the assemblage is often comprised of both foraminifera and thecamoebians in varying abundances. In these environments, distinguishing salinity can often be difficult as many other factors such as nutrient loading, pH, and dissolved oxygen also play a significant role. Coastal anchialine cave systems, like those found in the Yucatan, provide a new unique environment in which to study foraminiferal and thecamoebian transitions in low salinities. They are permanently aquatic and much more stable than traditional intertidal habitats, and due to their sheltered nature microfossils in these environments are less subject to taphonomic processes (e.g. wave action, diagenesis).

The results from the Ox Bel Ha cave system provide further evidence that thecamoebians and foraminifera exist in a variety of anchialine cave environments and that they show significant faunal transitions along a shore-normal transect in response to changing salinities and hydrochemical parameters, such as dissolved oxygen. Caution must be taken when interpreting the faunal assemblages as there may be significant bias as a result of long-term time averaging. Further documentation of the population changes in other anchialine cave systems on the Yucatan and elsewhere in the world will greatly help in understanding the ecologic controls on these unique habitats.

ACKNOWLEDGEMENTS

We gratefully acknowledge Francisco Hernandez Franco, Encargado de la Sémarnat (Quintana Roo); Gustavo Maldonado Saldaña, Director of Secretaria del Medio Ambiente y Ecología for the municipality of Solidaridad; Paul Sánchez-Navarro of Centro Ecológico Akumal; diving logistics and sampling from The Mexico Cave Exploration Project and Cindaq (F. Devos, C. Le Maillot, S. Meacham, and D. Riordan), and B. Wilson and E. Utigard for SCUBA support. Special thanks to F. Devos for drafting the cave map.

Funding was provided by The Royal Geographic Society (with The institute of British Geographers) Ralph Brown Expedition Award (EGR & PAB), National Geographic (Committee for Research and Exploration Grant; EGR & PAB), National Science and Engineering Research Council of Canada Post-Graduate Scholarship (PvH), and Discovery Grant (EGR); and Student Research Grants (to PvH) from: the Geological Society of America, the Cushman Foundation for Foraminiferal Research, and the Sigma Xi Scientific Research Society.

Appendix A – Benthic Microfossils Species List

Foraminifera

Ammodiscus tenuis (Grzybowski, 1898, p. 282, pl. 10, fig. 35)
Ammonia beccarii forma *tepida* (Cushman, 1926) – Hayward et al. 2003 p. 353, pl. 1, figs. 1-8
Elphidium spp. (Montfort, 1808)
Miliammina fusca (Brady, 1870, p. 47, pl. 11, figs. 2-3)
Physalidia simplex (Heron-Allen and Earland, 1928, pl. 1, figs. 1-2). Note: identified as *Ammonia tepida* var. juvenile in van Hengstum et al. (2008, 2009) and Gabriel et al. (2009)
Siphotrochammina lobata (Saunders, 1957)
Tiphotrocha comprimata (Cushman and Brönnimann) emend. Saunders, 1957
Triloculina oblonga (Montagu, 1803)
Trochammina macrescens (Brady, 1870) – Scott et al. 1991, p. 388, pl. 2, figs. 10-11

Testate Amoebae (thecamoebians)

Arcella vulgaris (Ehrenberg, 1830, p. 40, pl. 1, fig. 6)
Centropyxis aculeata (Ehrenberg, 1832a, p. 40)
Centropyxis constricta (Ehrenberg, 1843, p. 410, pl. 4, fig. 35)
Difflugia oblonga (Ehrenberg, 1832b, p. 90)

References

Back, W., Hanshaw, B. B., Herman, J. S., and Van Driel, J. N., 1986, Differential dissolution of a Pleistocene reef in the ground-water mixing zone of coastal Yucatan, Mexico: Geology, v. 14, p. 137-140.

Barbosa, C. F., 2000, Foraminifera and Arcellacea ("Thecamoebians") zonation in South Brazilian mangroves: Proceedings of a Symposium; Sustentabilidade de Estuarios e Manguezais: Desafios e Perspectivas. Recife, Brazil, 22-28 May, 2000.

Berkeley, A., Perry, C. T., Smithers, S. G., Horton, B. P., and Taylor, K. G., 2007, A review of the ecological and taphonomic controls on foraminiferal assemblage development in intertidal environments: Earth Science Reviews, v. 83, p. 205-230.

________, Perry, C. T., Smithers, S. G., and Horton, B. P., 2008, The spatial and vertical distribution of living (stained) benthic foraminifera from a tropical, intertidal environment, north Queensland, Australia: Marine Micropaleontology, v. 69, p. 240-261.

Beddows, P. A., 2004, Groundwater hydrology of a coastal conduit carbonate aquifer: Caribbean coast of the Yucatan Peninsula, Mexico. PhD Thesis, University of Bristol, UK, 303 p.

________, Smart, P. L., Whitaker, F. F., and Smith, S., 2007, Decoupled fresh-saline groundwater circulation of a coastal carbonate aquifer: spatial patterns of temperature and specific conductivity: Journal of Hydrogeology, v. 346, p. 18-32.

Blanchon, P., and Shaw, J., 1995, Reef drowning during the last deglaciation: evidence for catastrophic sea level rise and ice sheet collapse: Geology, v. 23, p. 4-8

________, Jones, B., and Ford, D. C., 2002, Discovery of a submerged relic reef and shoreline off Grand Cayman: further support for an early Holocene jump in sea level: Sedimentary Geology, v. 147, p. 253-270.

Brady, H. B., 1870. Foraminifera, *in*: Brady, G. S., Robertson, D., and Brady, H. B., (eds), The Ostracoda and Foraminifera of Tidal Rivers: Annals and Magazine of Natural History-Series v. 4, no. 6, p. 273-306.

Charman, D. J., Roe, H. M., and Gehrels, W. R., 2002, Modern distribution of saltmarsh testate amoebae: regional variability of zonation and response to environmental variables: Journal of Quaternary Science, v. 17(5-6), p. 387-409.

Cushman, J. A., 1926, Recent foraminifera from Puerto Rico: Publications of the Carnegie Institution of Washington, v. 342, p. 73-84.

Ehrenberg, G. C., 1830, Organisation, Systematik, und geographishers Verhältnis der Infusionsthierchen. Druckerei der Königliche Akademie der Wiessenschaften, Berlin

________, 1832a, Beiträge zue Kenntnis der Organisation der Infusorien und ihrer geographischen Verbreitung, besonders in Sibirien. Königliche

Akademie der Wiessenschaften zu Berlin Abhandlungen, 1830, Physikalische Klasse, 88 p.

________, 1832b, Über die Entwicklung und Lebensdauer der Infusionsthiere, nebst ferneren Beiträgen zu einer Vergleichung ihrer organischern System: Königliche Akademie der Wiessenschaften zu Berlin Abhandlungen, 1831, Physikalische Abhandlungen, 154 p.

________, 1843, Verbreitung und Einfluss des mikroskopischen lebens Süd- und Nord-Amerika. Königliche Akademie der Wiessenschaften zu Berlin Abhandlungen, Physikalische Abhandlungen, p. 291-446.

Gabriel, J. J., Reinhardt, E. G., Peros, M. C., Davidson, D. E., van Hengstum, P. J., and Beddows, P. A., 2009, Palaeoenvironmental evolution of Cenote Aktun Ha (Carwash) on the Yucatan Peninsula, Mexico and its response to Holocene sea-level rise: Journal of Paleolimnology, v. 42, no. 2, p. 199-213.

________, Reinhardt, E. G., van Hengstum, P. J., and Beddows, P. A., submitted, Late Holocene (3500 cal yBP) salinity changes and their climatic implications as recorded in an anchialine cave system, Ox Bel Ha, Yucatan, Mexico: (submitted to Journal of Paleolimnology).

Gehrels, W. R., Roe, H. M., and Charman, D. J., 2001, Foraminifera, testate amoebae and diatoms as sea level indicators in UK saltmarshes: a quantitative multiproxy approach: Journal of Quaternary Science, v. 16, no. 3, p. 201-220.

Grzybowski, J., 1898, Otwornice pokladów naftonosynch okolicy Krosna, Akad. Umiej. Krakowie, Wydz. Mat.-Przyr., Kraków, 1898, v. 33

Hammer, Ø., Harper, D. A. T., and Ryan, P. D., 2001, PAST: Paleontological statistics software package for education and data analysis: Palaeontologia Electronica, v. 4, no. 1, 9 p., http://palaeo-electronica.org/2001_1/past/issue1_01.htm.

Hanshaw, B. B., and Back, W., 1980, Chemical mass-wasting of the northern Yucatan by groundwater dissolution: Geology, v. 8, no. 5, p. 222-224.

Haug, G. H., Hughen, K. A., Sigman, D. M., Peterson, L. C., and Röhl, U. ,2001, Southward Migration of the Intertropical Convergence Zone Through the Holocene: Science, v. 293, p. 1304-1308.

Hayward, B. W., Buzas, M. A., Buzas-Stephens, P., and Holzmann, M., 2003, The lost types of *Rotalia beccarii* var. *tepida* Cushman 1926: Journal of Foraminiferal Research, v. 33, no. 4, p. 352-354.

Heron-Allen, E., and Earland, A., 1928, On the Pegididae, a new family of foraminifera: Royal Microscopical Society London, v. 48, no. 3, p. 288.

Hodell, D. A., Brenner, M., Curtis, J. H., and Guilderson, T. ,2001, Solar forcing of drought frequency in the Maya Lowlands: Science, v. 292, p. 1367-1370.

Horton, B. P., and Culver, S. J., 2008, Modern Intertidal Foraminifera of the Outer Banks, North Carolina, U.S.A., and their Applicability for Sea-Level Studies: Journal of Coastal Research, v. 24, no. 5, p. 1110-1125.

Iliffe, T. M., 1992, An annotated list of the troglobitic anchialine fauna and freshwater fauna of Quintana Roo: *in* Navarro, D., and Suárez-Morales, E. (eds), Diversidad Biologica en la Reserva de la Biosfera de Sian Ka'an Quintana Roo, Mexico, Volume 2: Centro de Investigaciones de Quintana Roo/Secretaria de Desarrollo Social, Chetumal, p. 197-215.

Javaux, E. J., and Scott, D. B., 2003, Illustration of Modern Benthic Foraminifera from Bermuda and Remarks on Distribution in Other Subtropical/tropical Areas: Palaeontologia Electronica, v. 6, no. 4, 29 p., http://palaeo-electronica.org/paleo/2003_1/benthic/issue1_03.htm.

Maddocks, R. F., 2005, New thalassocypridine Ostracoda from anchialine caves of the Loyalty Islands, New Caledonia (Podocopida, Paracypridinae): Micropaleontology, v. 51, p. 169-216.

Medioli, F. S., and Scott, D. B., 1983, Holocene Arcellacea (Thecamoebians) from Eastern Canada: Cushman Foundation Special Publication No. 21, 63 p.

Mejia-Ortiz, L., Yanez, G., Lopez-Mejia, M., and Zarza-Gonzalez, E., 2007, Cenotes (anchialine caves) on Cozumel Island, Quintana Roo, Mexico: Journal of Cave and Karst Studies, v. 69, no. 2, p. 250-255.

Montfort, D., 1808, Conchyliologie systématique et classification méthodique de coquilles. Paris, France, 15 p.

Montagu, G., 1803, Testacea Britannica, or natural history of British shells, marine, land, and fresh-water, including the most minute. J.S. Hollis, Romsey, England, p. 1 – 606.

Moore, Y. H., Stoessell, R. K., and Easley, D. H., 1992, Fresh-water/sea-water relationship within a groundwater system, northeastern coast of the Yucatan Peninsula: Ground Water, v. 30, p. 343-350.

Murray, J., 2006, Ecology and Applications of Benthic Foraminifera: Cambridge University Press, New York, 426 p.

Namiotko, T., Wouters, K., Danielopol, D. L., and Humphreys, W. F., 2004, On the origin and evolution of a new anchialine stygobitic Microceratina species (Crustacea, Ostracoda) from Christmas Island (Indian Ocean): Journal of Micropalaeontology, v. 23, no. 1, p. 49-59.

Patterson, R. T., and Kumar, A., 2002, A review of current testate rhizopod (thecamoebian) research in Canada: Palaeogeography, Palaeoclimatology, Palaeoecology, v. 180, p. 225-251.

Perry, E., Swift, J., Gamboa, J., Reeve, A., Sanborn, R., Marín, L. E., and Villasuso, M., 1989, Geologic and environmental aspects of surface cementation, north coast, Yucatan, Mexico: Geology, v. 17, p. 818-821.

Quintana Roo Speleological Society (QRSS),11 September 2009, List of long underwater caves in Quintana Roo, Mexico [Online]. Available: http://www.caves.org/project/qrss/qrlong.htm [Accessed online 28 Nov 2009].

Reinhardt, E. G., Dalby, A. P., Kumar, A., and Patterson, R. T., 1998, Arcellaceans as pollution indicators in mine tailing contaminated lakes near Cobalt, Ontario, Canada: Micropaleontology, v. 44, no. 2, p. 131-148.

Riveiros, N. V., Babalola, A. O., Boudreau, R. E. A., Patterson, R. T., Roe, H. M., and Doherty, C., 2007, Modern distribution of salt marsh foraminifera and thecamoebians in the Seymour-Belize Inlet Complex, British Columbia, Canada: Marine Geology, v. 242, p. 39-63.

Sánchez, M., Alcocer, J., Escobar, E., and Lugo, A., 2002, Phytoplankton of cenotes and anchialine caves along a distance gradient from the northeastern coast of Quintana Roo, Yucatan Peninsula: Hydrobiologia, v. 467, p. 79-89.

Saunders, J. B., 1957, Trochamminidae and certain Lituolidae (Foraminifera) from the recent brackish-water sediments of Trinidad, British West Indies: Smithsonian Miscellaneous Collections, v. 134, p. 1-16.

Schmitter-Soto, J. J., Comin, F. A., Escobar-Briones, E., Herrera-Silveira, J., Alcocer, J., Suárez-Morales, E., Elías-Gutiérrez, M., Díaz-Arce, V., Marín, L. E., and Steinich, B., 2002, Hydrogeochemical and biological characteristics of cenotes in the Yucatan Peninsula (SE Mexico): Hydrobiologia, v. 467, 215-228.

Scott, D. B., and Medioli, F. S., 1980, Living vs. total foraminiferal populations: their relative usefulness in paleoecology: Journal of Paleontology, v. 54, no. 4, p. 814-831.

________, and Hermelin, J. O. R., 1993, A device for precision splitting of micropaleontological samples in liquid suspension: Journal of Paleontology, v. 67, p. 151-154.

________, Medioli, F. S., and Schafer, C. T., 2001, Monitoring in Coastal Environments Using Foraminifera and Thecamoebians: Cambridge University Press, Cambridge, UK. 172 pp.

Smart, P. L., Dawans, J. M., and Whitaker, F., 1988, Carbonate dissolution in a modern mixing zone: Nature, v. 335, p. 811-813.

________, Beddows, P. A., Coke, J., Doerr, S., Smith, S., and Whitaker, F. F., 2006. Cave development on the Caribbean coast of the Yucatan Peninsula, Quintana Roo, Mexico: Geological Society of America Special Paper No. 404, p. 105-128.

Szabo, B. J., Ward, W. C., Weidie, A. E., and Brady, M. J., 1978, Age and magnitude of the late Pleistocene sea-level rise of the eastern Yucatan Peninsula: Geology, v. 6, p. 713-715.

Taylor, P.M., and Chafetz, H. S., 2004, Floating rafts of calcite crystals in cave pools, Central Texas, U.S.A.: Crystal Habit vs. Saturation State: Journal of Sedimentary Research, v. 74, no. 3, p. 328-341.

Usera, J., Blázquez, A. M., Guillem, J., and Alberola, C., 2002, Biochronological and paleoenvironmental interest of foraminifera lived in restricted environments: applications to the study of the western Mediterranean Holocene: Quaternary International, v. 93-94, p. 139-147.

Vacher, H. L., and Wallis, T. N., 1992, Comparative hydrogeology of fresh-water lenses of Bermuda and Great Exuma Island, Bahamas: Ground Water, v. 30, no. 1, p. 15-20.

________, and Mylroie, J. E., 2002, Eogenetic karst from the perspective of an equivalent porous medium: Carbonates and Evaporites, v. 17, no. 2, p. 182-196.

van Hengstum, P. J., Reinhardt, E. G., Beddows, P. A., Huang, R. J., and Gabriel, J. J., 2008, Thecamoebians (Testate Amoebae) and Foraminifera from three anchialine cenotes in Mexico: Low Salinity (1.5-4.5 psu) faunal transitions: Journal of Foraminiferal Research, v. 38, no. 4, p. 305-317.

________, ________, ________, Schwarcz, H. P., and Gabriel, J. J., 2009, Foraminifera and testate amoebae (thecamoebians) in an anchialine cave: Surface distributions from Aktun Ha (Carwash) cave system, Mexico: Limnology and Oceanography, v. 54, no. 1, p. 391-396.

________, ________, ________, and Gabriel, J. J., in press, Investigating linkages between Holocene paleoclimate and paleohydrogeology in Mexican anchialine cave sediments: Quaternary Science Reviews.

Weidie, A. E., 1985, Geology of the Yucatan Platform, *in* Ward, W. C., Weidie, A. E., and Back, W. (eds.), Geology and Hydrogeology of the Yucatan and Quaternary Geology of the Northeastern Yucatan Peninsula: New Orleans Geological Survey Field Trip Guide, p. 1-19.

Figure Captions

Figure 1: The location of Ox Bel Ha on the Yucatan Peninsula, Mexico

Figure 2: An interpretive diagram showing the nature of the groundwater aquifer on the Caribbean coast of the Yucatan Peninsula along a shore-normal transect. Cenote Aktun Ha is the only other cave system in the region that has been the subject of surface distributions of microfossils in an anchialine cave (van Hengstum and others, 2009).

Figure 3: Cave map of the lower reaches of Ox Bel Ha and the sample locations. Map drafted by F. Devos.

Figure 4: Hydrologic profiles of the water column from Tarpon I, Little Chen, and Arizona. The shaded region represents the two haloclines.

Figure 5: A Q-mode dendrogram indicating six distinct assemblages. The mean depth, salinity and Shannon diversity index, with 1 standard deviation, are provided for each assemblage.

Figure 6: A ternary diagram showing the relative abundance of thecamoebians and foraminifera in the assemblages. The black arrow indicates the expected trend for increasing salinity.

Plate 1: **1-14** Foraminifera: **1** *Ammonia tepida*, spiral side; **2** *A. tepida*, umbilical side; **3 - 4** *Elphidium excavatum*; **5** *E. gunteri*; **6 - 7** *Physalidia simplex*; **8** *Triloculina oblonga*; **9** *Ammodiscus tenuis*; **10** *Miliammina fusca*; **11 – 12** *Tiphotrocha comprimata* – note the "T" shaped final chamber in the umbilical view; **13 – 14** *Siphotrochammina lobata*; **15 – 20** Thecamoebians: **15** *Centropyxis aculeata* "aculeata"; **16** *C. aculeata* "discoides"; **17** *Difflugia oblonga*; **18** *Arcella vulgaris*; **19** *Centropyxis constricta* "spinosa"; **20** *C. constricta* "aerophile". Scale bars represent 50 µm.

Table 1: Relative fractional abundance and standard error ($\pm 1\sigma$) for taxonomic units

Sample	SS1	SS2	SS3	SS4	SS5	SS6	SS7	SS8	SS9	SS10
Depth (m)	7.6	7.8	9.2	7.9	9.2	8.5	7.6	7.7	7	9.1
Salinity (ppt)	6.33	5.66	5.66	5.68	5.66	5.67	5.66	5.66	5.66	5.66
Total Specimens	221	419	332	283	357	212	437	411	285	236
Individuals/cc	707.2	2681.6	2124.8	1811.2	2284.8	5427.2	2796.8	2630.4	1824	1510.4
Shannon diversity index	2.14	1.344	1.336	1.577	1.628	1.148	1.588	1.149	1.873	1.986
Arcella vulgaris	1.36	-	-	0.71	-	-	0.92	-	1.00	1.63
standard error (+/-)	1.53	-	-	0.98	-	-	0.89	-	1.16	1.62
Centropyxis aculeata "aculeata"	2.71	0.95	7.53	2.83	1.68	-	1.14	0.49	3.01	7.35
standard error (+/-)	2.14	0.93	2.84	1.93	1.33	-	1.00	0.67	1.98	3.33
C. aculeata "discoides"	2.71	1.91	3.01	2.47	2.24	0.47	1.60	0.73	3.01	2.86
standard error (+/-)	2.14	1.31	1.84	1.81	1.54	0.92	1.18	0.82	1.98	2.13
C. constricta "spinosa"	11.31	3.58	3.01	18.02	7.84	2.83	9.61	0.73	24.08	31.84
standard error (+/-)	4.18	1.78	1.84	4.48	2.79	2.23	2.76	0.82	4.96	5.94
C. constricta "aerophile"	8.60	3.58	3.61	8.13	7.84	2.36	6.64	1.95	11.71	16.33
standard error (+/-)	3.70	1.78	2.01	3.18	2.79	2.04	2.33	1.34	3.73	4.72
Difflugia oblonga	-	-	-	-	-	-	-	-	-	-
standard error (+/-)	-	-	-	-	-	-	-	-	-	-
Ammodiscus tenuis	-	-	-	-	-	-	-	-	-	-
standard error (+/-)	-	-	-	-	-	-	-	-	-	-
Ammonia tepida	31.67	57.76	65.66	48.41	49.86	67.92	51.26	71.29	37.79	21.63
standard error (+/-)	6.13	4.73	5.11	5.82	5.19	6.28	4.69	4.37	5.63	5.25
Elphidium excavatum	7.69	0.24	1.51	0.35	1.68	14.15	3.43	3.16	0.33	1.22
standard error (+/-)	3.51	0.47	1.31	0.69	1.33	4.69	1.71	1.69	0.67	1.40
Elphidium gunteri	9.05	2.86	4.22	0.71	1.68	6.60	13.96	6.08	1.34	2.86
standard error (+/-)	3.78	1.60	2.16	0.98	1.33	3.34	3.25	2.31	1.33	2.13
Haplophragmoides wilberti	1.36	0.48	-	0.35	-	-	0.69	0.73	-	-
standard error (+/-)	1.53	0.66	-	0.69	-	-	0.77	0.82	-	-
Helenina andersoni	-	-	-	-	-	-	1.14	0.00	-	-
standard error (+/-)	-	-	-	-	-	-	1.00	0.00	-	-
Miliammina fusca	5.43	23.15	-	13.43	19.33	2.36	3.20	5.60	5.35	2.45
standard error (+/-)	2.99	4.04	-	3.97	4.10	2.04	1.65	2.22	2.61	1.97
Physalidia simplex	-	-	2.71	-	-	-	-	0.24	-	-
standard error (+/-)	-	-	1.75	-	-	-	-	0.48	-	-
Siphotrochammina lobata	8.60	2.39	2.11	3.89	4.76	0.47	4.35	1.70	4.68	3.67
standard error (+/-)	3.70	1.46	1.55	2.25	2.21	0.92	1.91	1.25	2.45	2.40
Tiphotrocha comprimata	6.79	2.39	-	-	1.12	2.83	0.92	6.81	1.67	0.82
standard error (+/-)	3.32	1.46	-	-	1.09	2.23	0.89	2.44	1.49	1.15
Trochammina macrescens	2.71	0.72	5.42	0.71	1.96	-	-	0.49	6.02	7.35
standard error (+/-)	2.14	0.81	2.44	0.98	1.44	-	-	0.67	2.76	3.33
Triloculina oblonga	-	-	1.20	-	-	-	1.14	-	-	-
standard error (+/-)	-	-	1.17	-	-	-	1.00	-	-	-

Sample	SS11	SS12	SS13	SS14	SS15	SS16	SS17	SS18	SS19	SS20
Depth (m)	8.2	8.8	9.5	13.1	6.7	12.5	13.7	13.1	13.1	14.3
Salinity (ppt)	5.67	5.67	6.03	16.4	5.72	16.39	16.4	16.4	16.4	16.4
Total Specimens	390	241	201	256	199	179	211	331	388	152
Individuals/cc	19968	1542.4	1286.4	819.2	424.53	572.8	675.2	1059.2	310.4	486.4
Shannon diversity index	1.329	1.797	1.835	2.434	2.264	2.328	2.140	2.184	1.600	1.961
Arcella vulgaris	-	1.21	0.97	4.44	-	1.63	10.09	5.90	0.51	2.63
standard error (+/-)	-	1.38	1.36	2.52	-	1.86	4.06	2.54	0.71	2.54
Centropyxis aculeata "aculeata"	-	2.82	0.97	3.07	6.55	7.07	7.80	7.37	9.21	12.50
standard error (+/-)	-	2.09	1.36	2.11	3.44	3.75	3.62	2.82	2.88	5.26
C. aculeata "discoides"	-	4.84	1.94	9.56	2.18	12.50	5.05	4.13	5.37	13.82
standard error (+/-)	-	2.71	1.91	3.60	2.03	4.84	2.95	2.14	2.24	5.49
C. constricta "spinosa"	0.50	14.92	3.40	16.38	15.28	9.24	25.23	15.93	13.04	33.55
standard error (+/-)	0.70	4.50	2.50	4.53	5.00	4.24	5.86	3.94	3.35	7.51
C. constricta "aerophile"	0.25	6.45	3.40	13.99	5.68	9.78	11.93	12.68	4.09	13.16
standard error (+/-)	0.50	3.10	2.50	4.25	3.22	4.35	4.37	3.59	1.97	5.37
Difflugia oblonga	-	-	-	-	-	-	0.92	-	0.77	1.32
standard error (+/-)	-	-	-	-	-	-	1.29	-	0.87	1.81
Ammodiscus tenuis	-	-	-	-	-	2.72	0.46	0.59	-	-
standard error (+/-)	-	-	-	-	-	2.38	0.91	0.83	-	-
Ammonia tepida	52.13	32.66	18.93	7.51	21.83	22.83	20.18	24.78	52.43	7.89
standard error (+/-)	4.96	5.92	5.42	3.23	5.74	6.15	5.42	4.65	4.97	4.29
Elphidium excavatum	11.28	-	2.43	-	2.62	-	-	-	-	-
standard error (+/-)	3.14	-	2.13	-	2.22	-	-	-	-	-
Elphidium gunteri	25.56	1.61	4.37	4.44	8.73	7.07	2.29	7.08	0.51	-
standard error (+/-)	4.33	1.59	2.83	2.52	3.92	3.75	2.02	2.76	0.71	-
Haplophragmoides wilberti	-	-	-	-	-	-	-	1.77	-	-
standard error (+/-)	-	-	-	-	-	-	-	1.42	-	-
Helenina andersoni	-	-	-	-	-	2.72	3.21	2.36	0.77	-
standard error (+/-)	-	-	-	-	-	2.38	2.38	1.64	0.87	-
Miliammina fusca	0.25	28.63	46.12	3.75	2.62	8.15	0.92	4.13	0.77	-
standard error (+/-)	0.50	5.71	6.89	2.33	2.22	4.01	1.29	2.14	0.87	-
Physalidia simplex	-	-	-	0.68	-	1.09	2.29	2.06	2.05	2.63
standard error (+/-)	-	-	-	1.01	-	1.52	2.02	1.53	1.41	2.54
Siphotrochammina lobata	2.26	2.82	9.22	12.63	13.10	5.43	5.96	7.96	9.21	7.24
standard error (+/-)	1.47	2.09	4.00	4.07	4.69	3.32	3.20	2.92	2.88	4.12
Tiphotrocha comprimata	5.51	0.40	5.34	6.14	2.62	4.89	2.29	1.47	1.28	-
standard error (+/-)	2.27	0.80	3.11	2.94	2.22	3.16	2.02	1.30	1.12	-
Trochammina macrescens	2.26	2.82	2.43	16.38	16.16	4.89	1.38	1.77	-	5.26
standard error (+/-)	1.47	2.09	2.13	4.53	5.11	3.16	1.57	1.42	-	3.55
Triloculina oblonga	-	0.81	0.49	1.02	2.62	-	-	-	-	-
standard error (+/-)	-	1.13	0.96	1.23	2.22	-	-	-	-	-

Sample	SS21	SS22	SS23	SS24	SS25	SS26	SS27	SS28	SS29	SS30
Depth (m)	14	12.8	9.5	10.4	10.7	10.6	15.2	14.5	16.1	9.8
Salinity (ppt)	16.4	16.4	6.03	15.73	16.21	16.25	31.77	17.84	33.77	5.61
Total Specimens	346	264	292	213	205	207	181	220	57	275
Individuals/cc	1107.2	844.8	934.4	681.6	328	441.6	144.8	469.33	45.6	586.67
Shannon diversity index	2.346	2.002	1.575	1.455	2.250	2.256	2.033	1.936	1.588	1.853
Arcella vulgaris	6.53	6.84	3.42	-	5.37	4.89	6.74	4.09	1.69	3.27
standard error (+/-)	2.60	3.05	2.09	-	3.08	2.94	3.65	2.62	3.35	2.10
Centropyxis aculeata "aculeata"	10.23	14.45	3.42	0.94	2.44	5.78	11.80	7.27	3.39	2.55
standard error (+/-)	3.19	4.24	2.09	1.30	2.11	3.18	4.70	3.43	4.70	1.86
C. aculeata "discoides"	2.84	7.60	3.08	0.94	4.39	2.22	3.93	2.73	1.69	5.09
standard error (+/-)	1.75	3.20	1.98	1.30	2.80	2.01	2.83	2.15	3.35	2.60
C. constricta "spinosa"	21.59	24.33	9.25	2.35	11.71	15.11	10.67	14.09	15.25	14.55
standard error (+/-)	4.34	5.18	3.32	2.03	4.40	4.88	4.50	4.60	9.33	4.17
C. constricta "aerophile"	6.53	17.87	4.45	0.94	7.32	1.78	2.25	5.00	1.69	9.82
standard error (+/-)	2.60	4.62	2.37	1.30	3.56	1.80	2.16	2.88	3.35	3.52
Difflugia oblonga	6.53	1.52	2.40	0.94	0.49	-	-	-	-	-
standard error (+/-)	2.60	1.48	1.75	1.30	0.95	-	-	-	-	-
Ammodiscus tenuis	1.70	-	-	13.15	-	0.89	11.24	-	6.78	-
standard error (+/-)	1.36	-	-	4.54	-	1.28	4.60	-	6.53	-
Ammonia tepida	9.66	16.73	58.56	9.86	22.93	16.44	33.71	30.91	23.73	5.09
standard error (+/-)	3.11	4.50	5.65	4.00	5.75	5.05	6.89	6.11	11.04	2.60
Elphidium excavatum	-	-	-	-	-	0.89	-	-	-	-
standard error (+/-)	-	-	-	-	-	1.28	-	-	-	-
Elphidium gunteri	5.11	0.38	1.03	-	9.76	3.56	3.37	-	1.69	41.82
standard error (+/-)	2.32	0.74	1.16	-	4.06	2.52	2.63	-	3.35	5.83
Haplophragmoides wilberti	-	-	0.68	-	-	-	-	-	-	-
standard error (+/-)	-	-	0.95	-	-	-	-	-	-	-
Helenina andersoni	1.70	-	0.00	-	-	-	-	-	3.39	-
standard error (+/-)	1.36	-	0.00	-	-	-	-	-	4.70	-
Miliammina fusca	-	0.76	3.42	59.62	16.10	28.89	-	0.45	-	8.00
standard error (+/-)	-	1.05	2.09	6.59	5.03	6.17	-	0.89	-	3.21
Physalidia simplex	5.68	-	-	2.82	0.98	1.33	1.12	0.45	40.68	-
standard error (+/-)	2.44	-	-	2.22	1.35	1.56	1.54	0.89	12.75	-
Siphotrochammina lobata	14.49	4.56	7.53	4.69	8.29	8.00	6.18	15.91	-	4.36
standard error (+/-)	3.71	2.52	3.03	2.84	3.78	3.70	3.51	4.83	-	2.41
Tiphotrocha comprimata	5.68	0.76	1.37	2.82	6.83	2.22	8.99	16.82	-	1.09
standard error (+/-)	2.44	1.05	1.33	2.22	3.45	2.01	4.17	4.94	-	1.23
Trochammina macrescens	1.70	2.66	1.37	0.94	2.93	8.00	-	2.27	-	2.18
standard error (+/-)	1.36	1.94	1.33	1.30	2.31	3.70	-	1.97	-	1.73
Triloculina oblonga	-	1.52	-	-	0.49	-	-	-	-	2.18
standard error (+/-)	-	1.48	-	-	0.95	-	-	-	-	1.73

Sample	SS31	SS32	SS33	SS34	SS35	SS36	SS37
Depth (m)	6.7	7.7	15.2	9.1	18.6	22	18.5
Salinity (ppt)	5.7	5.7	31.77	6.3	35	35	35
Total Specimens	287	347	239				
Individuals/cc	612.27	2220.8	764.8	NO SIGNIFICANT RECOVERY			
Shannon diversity index	1.825	1.617	1.712				
Arcella vulgaris	12.89	4.90	7.11	-	-	-	-
standard error (+/-)	3.88	2.27	3.26	-	-	-	-
Centropyxis aculeata "aculeata"	2.44	2.59	2.09	-	-	-	-
standard error (+/-)	1.78	1.67	1.81	-	-	-	-
C. aculeata "discoides"	5.23	2.02	7.53	-	-	-	-
standard error (+/-)	2.57	1.48	3.35	-	-	-	-
C. constricta "spinosa"	5.57	14.99	25.10	-	-	-	-
standard error (+/-)	2.65	3.76	5.50	-	-	-	-
C. constricta "aerophile"	17.07	4.32	12.97	-	-	-	-
standard error (+/-)	4.35	2.14	4.26	-	-	-	-
Difflugia oblonga	-	-	-	-	-	-	-
standard error (+/-)	-	-	-	-	-	-	-
Ammodiscus tenuis	-	-	-	-	-	-	-
standard error (+/-)	-	-	-	-	-	-	-
Ammonia tepida	2.44	53.60	37.24	-	-	-	-
standard error (+/-)	1.78	5.25	6.13	-	-	-	-
Elphidium excavatum	0.70	-	-	-	-	-	-
standard error (+/-)	0.96	-	-	-	-	-	-
Elphidium gunteri	43.55	0.29	-	-	-	-	-
standard error (+/-)	5.74	0.56	-	-	-	-	-
Haplophragmoides wilberti	-	-	-	-	-	-	-
standard error (+/-)	-	-	-	-	-	-	-
Helenina andersoni	-	-	-	-	-	-	-
standard error (+/-)	-	-	-	-	-	-	-
Miliammina fusca	1.39	3.46	-	-	-	-	-
standard error (+/-)	1.36	1.92	-	-	-	-	-
Physalidia simplex	-	-	1.26	-	-	-	-
standard error (+/-)	-	-	1.41	-	-	-	-
Siphotrochammina lobata	2.09	7.20	5.44	-	-	-	-
standard error (+/-)	1.66	2.72	2.88	-	-	-	-
Tiphotrocha comprimata	3.14	2.88	1.26	-	-	-	-
standard error (+/-)	2.02	1.76	1.41	-	-	-	-
Trochammina macrescens	3.48	3.46	-	-	-	-	-
standard error (+/-)	2.12	1.92	-	-	-	-	-
Triloculina oblonga	-	0.29	-	-	-	-	-
standard error (+/-)	-	0.56	-	-	-	-	-

Table 2: Average depth, salinity and Shannon diversity index (SDI) and relative abundance of dominant species for each of the six assemblages.

Assemblage	1	2	3	4	5	6
Depth (m)	8.8	9.8	8.3	16.1	12.0	12.0
Salinity (ppt)	6.7	10.9	5.7	33.8	17.8	13.3
SDI	1.44	1.84	1.84	1.59	2.06	2.16
THECAMOEBIANS						
Arcella vulgaris	< 1	2 ± 1	8 ± 3	2 ± 3	4 ± 2	5 ± 2
Centropyxis aculeata "aculeata"	3 ± 1	3 ± 2	2 ± 2	4 ± 5	6 ± 5	9 ± 4
C. aculeata "discoides"	2 ± 1	3 ± 2	5 ± 3	2 ± 3	5 ± 3	7 ± 3
C. constricta "spinosa"	8 ± 3	9 ± 4	10 ± 3	16 ± 9	**15 ± 5**	**25 ± 6**
C. constricta "aerophile"	4 ± 2	3 ± 2	13 ± 4	2 ± 3	9 ± 4	13 ± 4
FORAMINIFERA						
Ammonia tepida	**57 ± 5**	20 ± 5	4 ± 2	**25 ± 11**	**31 ± 6**	16 ± 5
Elphidium spp.	9 ± 3	3 ± 2	**43 ± 6**	2 ± 3	5 ± 2	5 ± 3
Physalidia simplex	0	< 1	0	**42 ± 13**	< 1	2 ± 1
Miliammina fusca	7 ± 2	**42 ± 6**	5 ± 2	0	5 ± 2	2 ± 1
Other agglutined taxa	7 ± 3	**14 ± 2**	8 ± 2	0	**17 ± 6**	**21 ± 3**

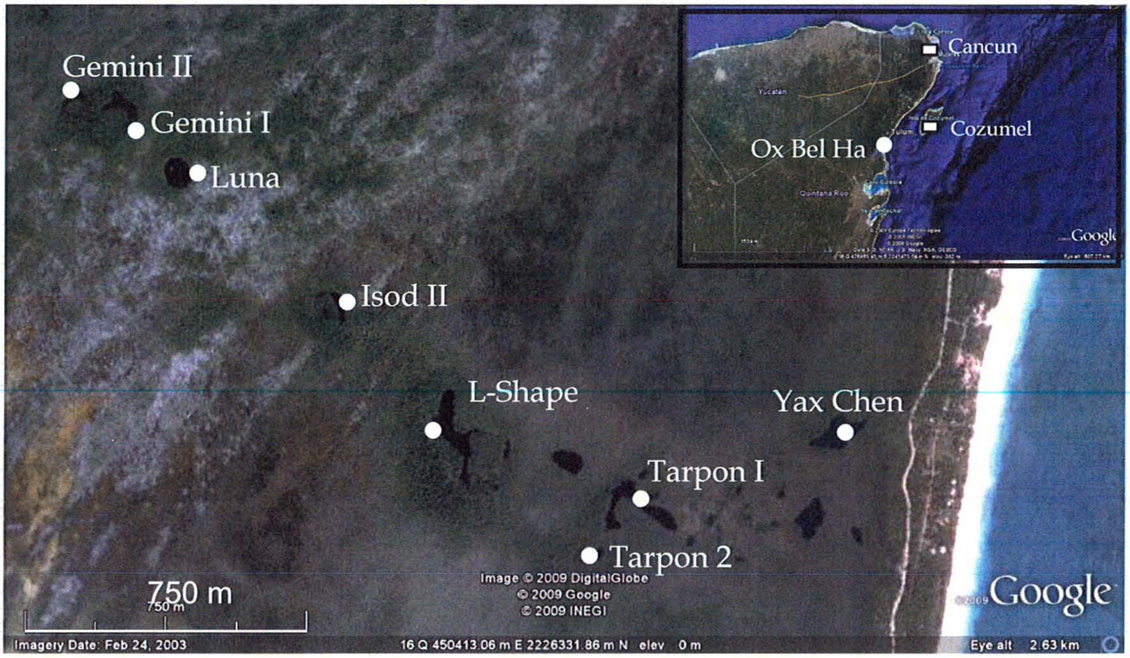
Gemini II
Gemini I
Luna
Isod II
L-Shape
Yax Chen
Tarpon I
Tarpon 2
Cancun
Cozumel
Ox Bel Ha
Yucatan
Tulum
Quintana Roo
750 m
Image © 2009 DigitalGlobe
© 2009 Google
© 2009 INEGI
©2009 Google
Imagery Date: Feb 24, 2003
16 Q 450413.06 m E 2226331.86 m N elev 0 m
Eye alt 2.63 km

Figure 1

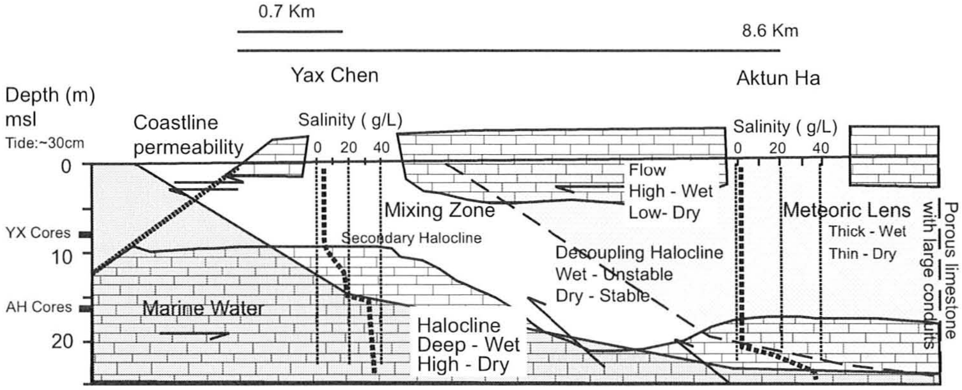
0.7 Km
8.6 Km
Yax Chen
Aktun Ha
Depth (m)
msl
Tide:~30cm
0
YX Cores
10
AH Cores
20
Coastline
permeability
Salinity (g/L)
0 20 40
Mixing Zone
Secondary Halocline
Marine Water
Halocline
Deep - Wet
High - Dry
Flow
High - Wet
Low- Dry
Decoupling Halocline
Wet - Unstable
Dry - Stable
Salinity (g/L)
0 20 40
Meteoric Lens
Thick - Wet
Thin - Dry
Porous limestone
with large conduits

Figure 2

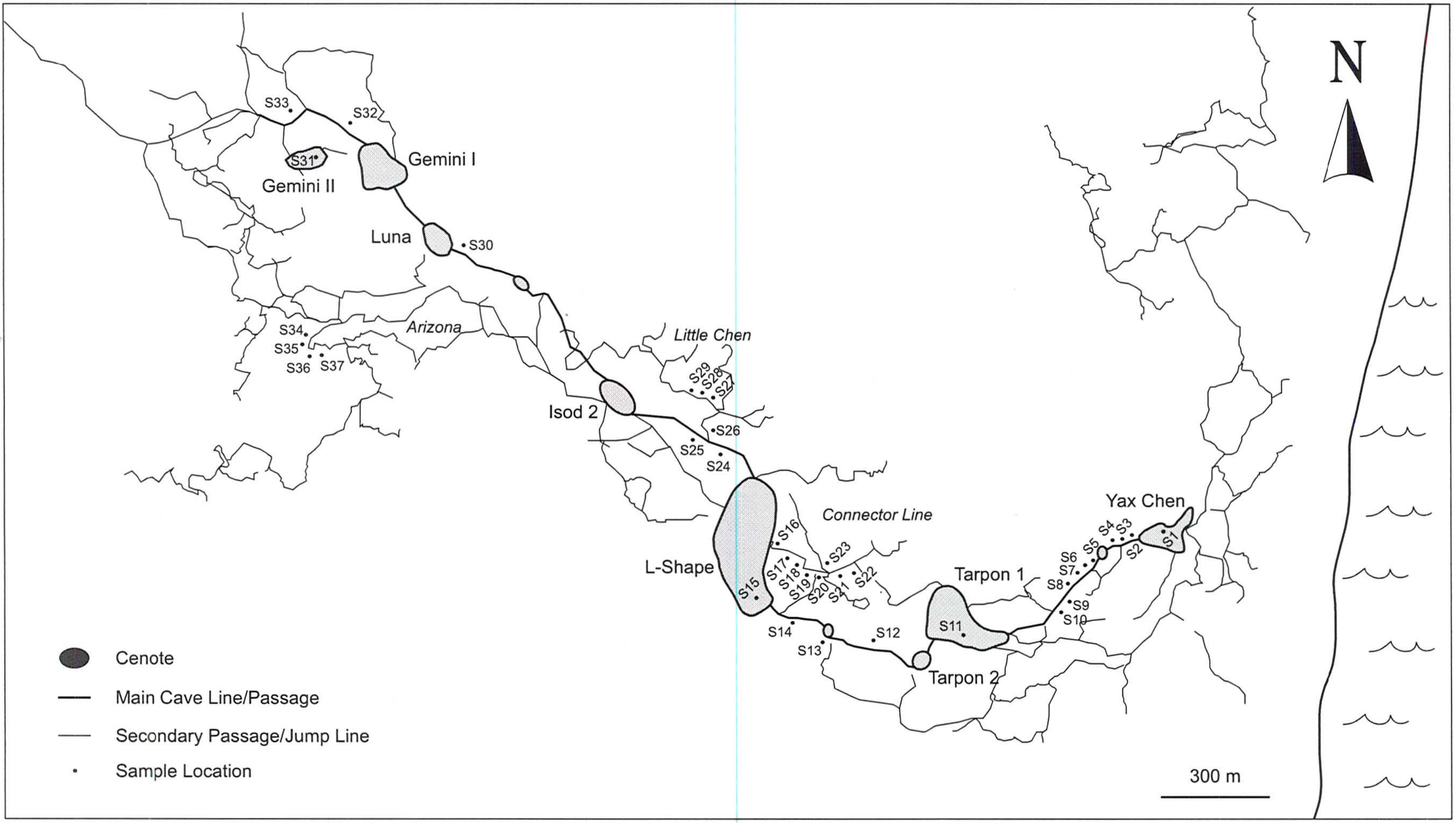
N
S33
S32
Gemini I
S31
Gemini II
Luna
S30
Arizona
S34
S35
S36
S37
Little Chen
S29
S28
S27
Isod 2
S26
S25
S24
Connector Line
L-Shape
S16
S15
S17
S18
S19
S20
S23
S21
S22
S14
S13
S12
Tarpon 1
S11
Tarpon 2
Yax Chen
S1
S2
S3
S4
S5
S6
S7
S8
S9
S10
300 m
Cenote
Main Cave Line/Passage
Secondary Passage/Jump Line
Sample Location

Figure 3

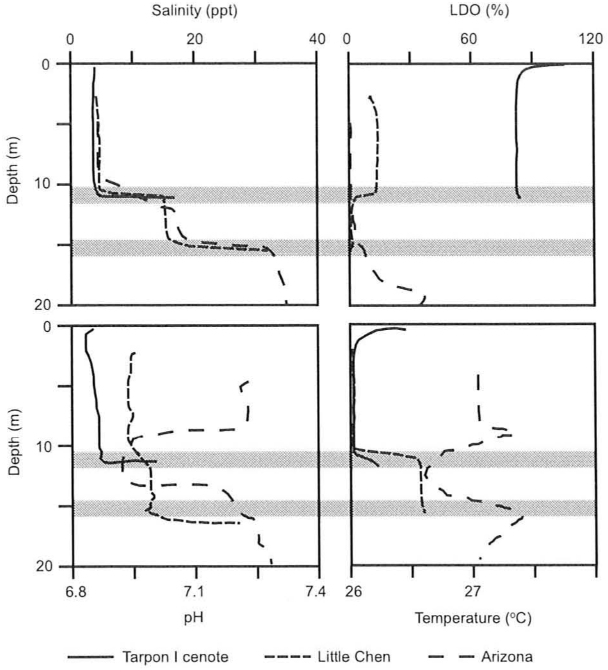
Salinity (ppt)
0
20
40
LDO (%)
0
60
120
Depth (m)
0
10
20
Depth (m)
0
10
20
6.8
7.1
7.4
pH
26
27
Temperature (°C)
Tarpon I cenote
Little Chen
Arizona

Figure 4

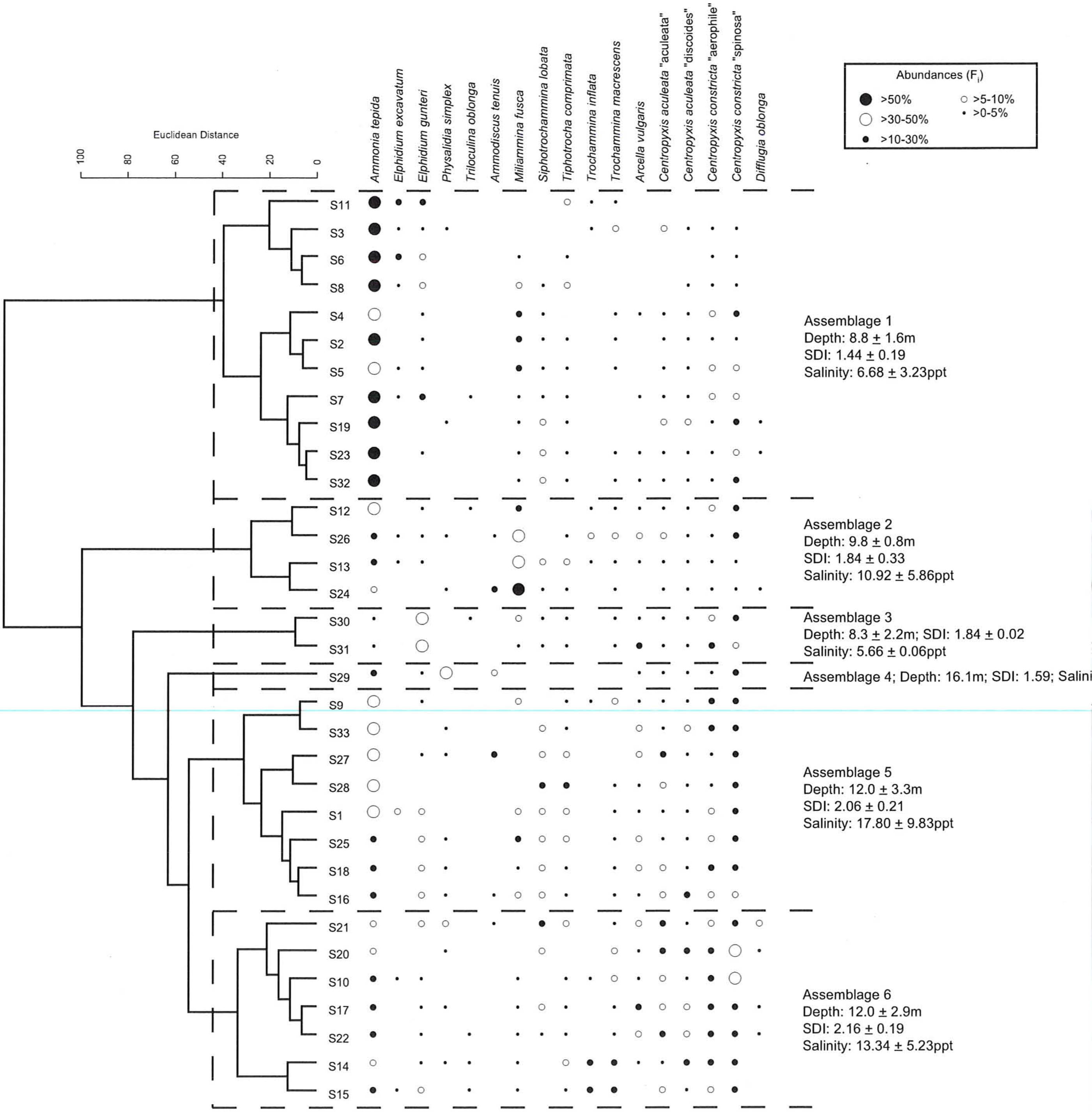
Euclidean Distance
100
80
60
40
20
0
Ammonia tepida
Elphidium excavatum
Elphidium gunteri
Physalidia simplex
Triloculina oblonga
Ammodiscus tenuis
Miliammina fusca
Siphotrochammina lobata
Tiphotrocha comprimata
Trochammina inflata
Trochammina macrescens
Arcella vulgaris
Centropyxis aculeata "aculeata"
Centropyxis aculeata "discoides"
Centropyxis constricta "aerophile"
Centropyxis constricta "spinosa"
Difflugia oblonga
Abundances (F_i)
>50%
>30-50%
>10-30%
>5-10%
>0-5%
S11
S3
S6
S8
S4
S2
S5
S7
S19
S23
S32
S12
S26
S13
S24
S30
S31
S29
S9
S33
S27
S28
S1
S25
S18
S16
S21
S20
S10
S17
S22
S14
S15
Assemblage 1
Depth: 8.8 ± 1.6m
SDI: 1.44 ± 0.19
Salinity: 6.68 ± 3.23ppt
Assemblage 2
Depth: 9.8 ± 0.8m
SDI: 1.84 ± 0.33
Salinity: 10.92 ± 5.86ppt
Assemblage 3
Depth: 8.3 ± 2.2m; SDI: 1.84 ± 0.02
Salinity: 5.66 ± 0.06ppt
Assemblage 4; Depth: 16.1m; SDI: 1.59; Salini
Assemblage 5
Depth: 12.0 ± 3.3m
SDI: 2.06 ± 0.21
Salinity: 17.80 ± 9.83ppt
Assemblage 6
Depth: 12.0 ± 2.9m
SDI: 2.16 ± 0.19
Salinity: 13.34 ± 5.23ppt

Figure 5

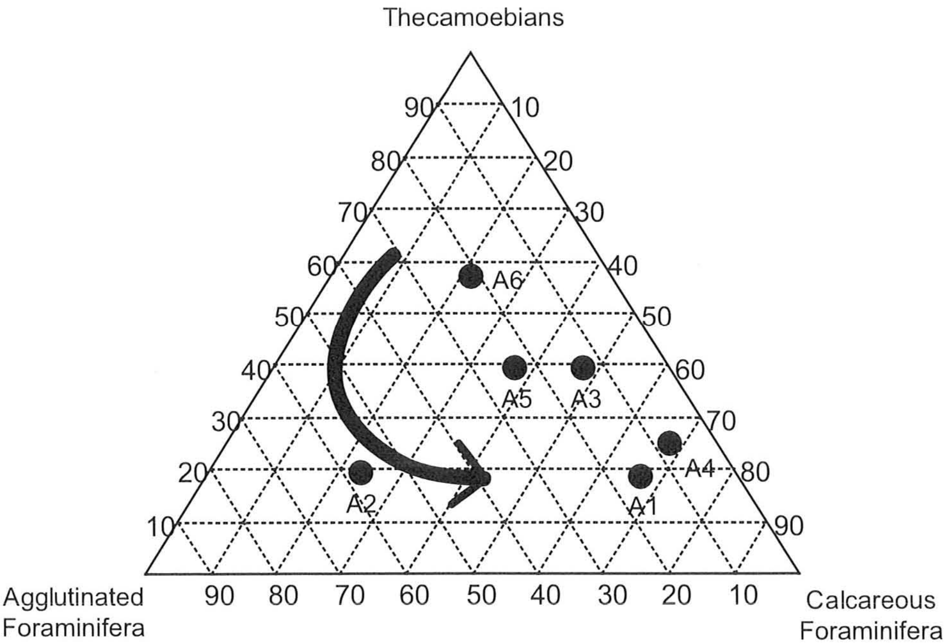
Thecamoebians
Agglutinated Foraminifera
Calcareous Foraminifera
90
80
70
60
50
40
30
20
10
10
20
30
40
50
60
70
80
90
90
80
70
60
50
40
30
20
10
A6
A5
A3
A4
A2
A1

Figure 6

Chapter 3

Late Holocene (3500 yBP) salinity changes and their climatic implications as recorded in an anchialine cave system, Ox Bel Ha, Yucatan, Mexico

Jeremy J. Gabriel, Eduard G. Reinhardt, Peter J. van Hengstum, and Patricia A. Beddows

This has been prepared for submission to Journal of Paleolimnology *and follows the formatting and referencing style of the journal.*

Abstract

Microfossil populations and organic geochemistry ($\delta^{13}C$ and $\delta^{15}N$, TOC, TN, and C/N ratio) were analyzed in four sediment cores collected from the lower (shoreward) area of the anchialine Ox Bel Ha cave system in the state of Quintana Roo, Mexico in order to reconstruct palaeoenvironmental changes through the late Holocene (< 3500 cal yBP). The cores were collected at 7.6 m and 9.2 m water depth along a shore-normal transect that extended up to 700 m from the coast. Four distinct environmental phases were identified. Phase 1 (4000 – 3000 cal yBP) is defined by calcareous foraminifera (*Ammonia tepida* and *Elphidium gunteri*) and thecamoebians (*Centropyxis* spp.) indicating highly variable precipitation patterns. Phase 2 (3000 – 1000 cal yBP) is characterized by an increased abundance of *A. tepida* and *E. gunteri* and a decrease of centropyxids indicating more saline conditions. The end of this phase corresponds to the Classic Period collapse of the ancient Maya. Phase 3 (1000 – 400 cal yBP) is marked by an increase in centropyxids indicating a freshening period, which is coincident with the start of the Post-Classic Period in Maya archaeology and the

founding of Tulum (~950 cal yBP), 8.5 km north of Ox Bel Ha. Phase 4 (400 – present) marks the onset of the modern salinity conditions (5 – 6 ppt) indicated by a decrease in centropyxids and an increase in *A. tepida*.

The environmental changes are closely linked to variations in precipitation patterns as a result of movement of the Intertropical Convergence Zone (ITCZ), increased strength and variability of the El Nino Southern Oscillation (ENSO), and global climatic events such as the Medieval Warm Period and the Little Ice Age. During times of increased precipitation there is more mixing of the groundwater which results in higher salinity within the cave and cenotes. Similarly, decreased precipitation results in increased stratification of the groundwater and a trend to fresher water. This relationship has important implications to understanding the relocation of the Maya during the Classic Period collapse and through the Post-Classic Period.

Introduction

The karst landscape of the Yucatan Peninsula, Mexico hosts extensive anastomosing phreatic cave systems that occupy an anchialine groundwater aquifer, consisting of basal marine water that is density-stratified from the superior freshwater. Cave systems such as these can be found in several global coastal locations such as islands in the Caribbean, the eastern and south Pacific Seas, and coastlines in the Mediterranean Sea (e.g. Maddocks, 2005; Namiotko et al., 2004; Smart et al., 1988). Scientific research in these environments has focused on the karst geology and hydrology (e.g. Smart et al., 2006; Moore et al., 1992; Hanshaw & Back, 1980), cave biology (e.g. Iliffe, 1992) and archaeology (Brady, 1997); however, it has only recently focussed on palaeoenvironmental evolution of the cave systems. Gabriel et al (2009) used a sediment core from the top of the collapse pile in Cenote Aktun Ha, Quintana Roo, Mexico to construct a 300-year record (~6800 – 6500 cal yBP) of the environmental changes within the cenote as a result of rising sea level in the Caribbean basin. Using the data from the cenote as well as analyzing three other cores obtained within the Aktun Ha cave system, van Hengstum et al (submitted) were able to extend the record from 6500 cal yBP to the present. By utilizing a multi-proxy approach of testate amoebae and foraminifera, organic stable isotopes ($\delta^{13}C$ and $\delta^{15}N$), total organic carbon and nitrogen, and the C/N ratio, this study focuses on the Ox Bel Ha cave system in Tulum, Quintana Roo, Mexico, and its environmental evolution in response to late Holocene climate change (Fig. 1A & B).

Background Research

Testate Amoebae and Foraminifera

Testate amoebae and foraminifera are single-celled protozoans that occupy virtually every fresh and marine aquatic environment, respectively. They form simple shells either through secretion of calcium carbonate (foraminifera) or polysaccharides (thecamoebians), or by agglutinating foreign particles together, both of which are readily preserved in all but the most extreme environments (e.g. low pH; Scott et al., 2001). Foraminifera have been used extensively in coastal reconstructions, including sea-level change (Kemp et al., 2009; Horton et al., 2007; Patterson et al., 2005), and their spatial distributions have been well documented in several coastal locations representing variable climates (Phleger, 1954; Ellison and Nichols, 1976; Scott et al., 1980). Testate amoebae (thecamoebians) have predominantly been used in lake and wetland studies to document characteristics such as pH, pollution, and land-use changes (Reinhardt et al., 2005; Patterson et al., 2002; Scott et al., 2001); however, when used in conjunction with foraminifera in estuarine environments they can be very effective indicators of hydrologic flow, temperature and salinity (Scott et al., 2001). There are currently very few studies that have analyzed the microfossil assemblages in flooded caves (e.g. van Hengstum et al., 2008, 2009; Javaux and Scott, 2003), and only three studies that have used microfossil assemblages to reconstruct palaeoenvironmental changes in caves and cenotes (Gabriel et al., 2009; van Hengstum et al., in press; Gabriel et al., submitted).

The dominant factor controlling the presence/absence of testate amoebae and foraminifera is salinity. *Ammonia* spp., which is generally considered one of the most euryhaline foraminifer taxa, requires a minimum salinity of 1-2 ppt while *Centropyxis* spp., the most euryhaline thecamoebian taxa, has an upper limit of ~3.5 ppt (van Hengstum et al., 2008, 2009). By looking at the transition between foraminifera- and thecamoebian-dominated populations, salinity changes can be inferred in low-salinity, brackish environments (van Hengstum et al., 2008, 2009; Riveiros et al., 2007; Patterson et al., 2005; Charman et al., 2002; Gehrels et al., 2001; Scott et al., 2001).

Climate Change and the Ancient Maya

The Maya civilization flourished for about 2000 years through much of eastern and southern Central America and was comprised of three main periods of cultural evolution: the Pre-Classic (4000-2000 yBP), the Classic (1900-1000 yBP), and the Post-Classic (1000-400 yBP). The extent of their civilization has been divided into three separate climatic regions: (1) The Pacific Plain (southern Guatemala and El Salvador), (2) the Southern and Central Lowlands (northern Guatemala, Honduras and Belize), and (3) the Northern Highlands (Yucatan Peninsula) (Sharer, 1994). Due to the high porosity of the limestone of the Yucatan Peninsula, meteoric rain water percolates immediately through the vadose zone and, as such, there are no surficial rivers and only a few lakes to store fresh water. The main access to fresh water for the Maya would have been through the cenotes, from the Yucatec Mayan word *dz'onot* (meaning "well"), making them an essential part to city-centres in the region. Some researchers (e.g. Johnston, 2004; Lucero, 2002) have suggested that the control of fresh water allowed Maya kings to maintain political power, and that the loss of water resources played a large role in the collapse of the Classic Maya.

Climate change in the region, particularly over the Late Holocene (< 3000 yrs), and its relation to the different phases of Maya evolution, has been the subject of a number of studies (e.g. Haug et al., 2003; Curtis et al., 1998; Hodell et al., 1995). The modern rainfall on the peninsula varies greatly on an east-west transect, with the Caribbean coast receiving up to 1400 mm/year while the northwest coast of the peninsula receives as little as 500 mm/year (from Hodell et al., 2005). Lake sediments from closed-system (i.e. no associated cave system) inland lakes have shown several cycles of drought through the late Holocene based on increased gypsum precipitation (Hodell et al., 1995), vegetation changes (Whitmore et al., 1996; Leyden 2002), and changes in $\delta^{18}O$ in carbonate shells (Curtis et al., 1998). Hodell et al (2001) concluded that the drought cycle has a dominant periodicity of 208 years and that some of the most severe drought cycles correspond to drastic declines in Maya populations. Indeed, the driest interval in the mid-late Holocene epoch occurred between 1300 and 1100 yBP (Hodell et al., 1995), which marks the end of the Classic period of Maya civilization and the abandonment of many of the most prominent city centres. There have been several causes for these climatic shifts including solar forcing (e.g. Hodell et al., 2001), migration of the Intertropical Convergence Zone (e.g. Haug et al., 2003) and well-known global climatic events such as the Little Ice Age and the Medieval Warm Period.

Holocene Sea-Level Rise

The late Pleistocene glaciation peaked about 18,000 years ago, with sea level in the Caribbean basin 121 $\pm$ 5 m below modern sea level (m.s.l.), as indicated by the shallow forming (< 5m) reef-crest coral *Acropora palmata* (Fairbanks, 1989). Subsequent sea-level rise due to melting of the glacial ice has varied through time in four main phases: (1) the late Pleistocene (17,000-12,500 yBP), which had rapid sea-level rise of ~0.4 m/100 yrs; (2) the Younger Dryas period (11,000-10,500 yBP), which has the lowest rates of sea-level rise (0.1 m/100yrs); (3) early

Holocene (9000-6000 yBP), with rates of 0.3 m/100 yrs; and (4) the late Holocene (6000-present), when sea-level rise started stabilizing and rate of rise decreased further to 0.1 m/100 yrs. Two additional phases have been identified, termed Meltwater Pulse 1A (12,000 yBP) and Meltwater Pulse 1B (9,500 yBP), when sea level rose 24 m and 28 m in less than 1000 years, respectively (Fairbanks, 1989). There is also evidence from Barbados and Grand Cayman Island reefs for a third phase of rapid rise (> 4.5 m/100 yrs) having occurred around 7,600 yBP (Blanchon & Shaw, 1995; Blanchon et al., 2002). Over the last 3500 years, sea-level rise in the Caribbean has been less than 1 metre (Blanchon & Shaw, 1995)

In addition to *A. palmata*, intertidal mangrove peat has been used to document Holocene sea-level rise (e.g. Ellison, 1993; Digerfeldt and Hendry, 1987). Toscano & Macintyre (2003) provided a calibrated sea-level curve for the Caribbean based on new and existing mangrove peat data. Though the water level range using mangrove peat is more confined than that of the reef-crest corals (~1 m) it is subject to wave erosion, compaction, and contamination of older, basal peat by younger peat accumulations (Gischler, 2006; Turetsky et al., 2004). Gabriel et al (2009) showed the utility of mangrove peat accumulations on the collapse pile of a cenote on the Yucatan Peninsula in reconstructing Holocene sea level in the Caribbean. These mangrove deposits are sheltered from wave and storm activity, accumulate on top of an elevationally stable collapse pile, and are better preserved in the extremely low energy environment of a flooded cenote. Results showed a distinct transition in the sediment record between the moist, terrestrial mangrove environment and the modern, flooded cenote conditions, which can be directly related to Caribbean sea level.

Study Area

The Yucatan Peninsula is a tectonically-stable carbonate platform comprised of Eocene (interior) to Quaternary (coastal) reefal limestone (Weidie, 1985; Szabo et al., 1978) with a density-stratified groundwater aquifer consisting of superior fresh meteoric water floating on top of encroaching basal seawater (Fig. 2). The limestone has a high primary porosity and is diagenetically immature making it more susceptible to dissolution than "telogenetic" continental karst environments (Smart et al., 2006; Vacher and Mylroie, 2002). In the brackish halocline, where the fresh and saline waters mix, the water is subsaturated in carbonates resulting in further dissolution (Back et al., 1986; Hanshaw and Back, 1980). Oscillations in Caribbean Sea levels through the Quaternary have shifted the relative level of the halocline resulting in the formation of long, anastomosing cave systems that occupy both the fresh and marine sections of the ground-water aquifer. This study focuses on the eastern section of the Ox Bel Ha cave system just outside of Tulum, Quintana Roo, Mexico (Fig. 1B), which is currently the longest underwater cave system in the world with 180 km of explored passage (QRSS, 2009). The first cenote in the system is Yax Chen, starting approximately 300 m from the modern Caribbean coastline. The cave system then runs in a northwestern transect, nearly perpendicular to the coast, and has several cenotes and smaller passages that connect to the main passage. There are two dominant haloclines found at ~10 m and ~14 m, although the fresher waters still have a moderate salinity of 6.2 ppt (Gabriel et al., submitted; see Fig. 2). Sediment accumulation, particularly that of organic matter, varies in relationship to proximity and size of the nearest upstream cenote. The ground-water velocity varies with distance from the coast because of the thickening of the fresh-water lens with velocities as high as 12 cm s^{-1} at coastal discharge sites and as low as 1 cm s^{-1} 10 km from the coast (Moore et al., 1992).

Cenote Yax Chen occupies the meteoric water mass (MW; 6.2 ppt, 25.9°C, and 7.1 mg L^{-1} dissolved oxygen) and is diamond-shaped with a long axis of ~140 m perpendicular to the coast, and a short axis of ~80 m. The bottom is covered in large part by massive limestone blocks that collapsed to form the cenote, although significant accumulations (> 1.5 m) of sediment can be found in many areas in between the blocks. There is no open conduit on the seaward side to directly connect this part of the system to the open ocean. It seems that meteoric water flowing seaward hits the beach head where it seeps through small fractures to the Caribbean Sea (Devos, Pers. Comm.). The cenote is about 8 km south of the ancient Maya city of Tulum, which was a coastal defence town that was occupied during the post-Classic period (~950 yBP; Sharer, 1994).

Methods

Four sediment push cores were obtained using 7.5 cm diameter polyvinyl tubing from separate locales, all within the MW in the Ox Bel Ha system, using SCUBA techniques in June 2007. The first core was taken from the open water cenote, Yax Chen (C1), from a depth of 7.5 m, two more cores were taken upstream of the cenote in the cavern zone (C2, C3; 9.2 m and 7.5 m, respectively), and the last one was taken from the cavern zone downstream of the cenote (C4, 7.5 m depth; see Fig. 1C). The cavern zone is defined as having a rock ceiling but still within the limits of light penetration, which is typically <60 m. In order to find a suitable location to take a core (i.e. enough sediment accumulation), a small polycarbonate probing rod was used to determine sediment thickness. The cores were capped and sealed underwater and transported out of the cave. On land, the cores were manually extruded and sampled at 1 cm intervals for further analysis.

Sub-samples were taken every 3-5 cm in each core and washed over a 125 m and a 45 m screen to retain and concentrate thecamoebian and foraminifer assemblages. The sediment was split and analyzed using standard techniques (Patterson and Fishbein, 1989; Scott and Hermelin, 1993) and thecamoebian and foraminifer taxonomy was identified on the basis of published information (Poag, 1981; Medioli and Scott, 1983; Loeblich and Tappan, 1998: van Hengstum et 2008, 2009). The species were plotted according to their relative fractional abundance (F_i) of the total population such that:

$$F_i = \frac{C_i}{N_i}$$

where C_i is the individual species count and N_i is the total population (thecamoebians and foraminifera). In addition, the standard error was calculated based on the relative fractional abundance to determine statistically significant species according to the equation:

$$S_{F_i} = 1.96\sqrt{\frac{F_i(1-F_i)}{N_i}}$$

Q-mode cluster analysis was performed on each core using the statistical freeware program *PAST* (Hammer et al., 2001). Ward's method of minimum variance was used along with a constrained incremental sum of squares (CONISS) to cluster sample intervals using a simple Euclidean distance coefficient. The results from the cluster analysis did not prove to be effective and were not included (see below for discussion).

Bulk organic matter was collected at regular intervals for isotopic analysis of $\delta^{13}C_{org}$ and $\delta^{15}N_{org}$, including total organic carbon (TOC) and total nitrogen (TN). Due to a lack of organic matter in the cenote core (C1), it was not analyzed for organic isotopes. The samples were reacted with a 10% HCl solution for 24 hours to oxidize any carbonate matter and then rinsed twice with distilled water. The samples were then dried in an oven at 67°C and ground to a homogenous powder with a mortal and pestle. Sub-samples weighing between 400 and 500 μg were placed in to a Costech elemental analyzer where they were combusted and analysed with a Delta Plus XP mass spectrometer. The results were compared against internal, IAEA and NIST standards (NBS21, ANU-Sucrose, with reproducibility on replicates equal to $\pm$0.2‰) and the ratios were expressed in standard delta notation (δ) in per mil (‰) against Vienna PeeDee Belemnite (VPDB).

Adult carapaces of the ostracod *Cytheridella ilosvayi* were picked from seven intervals in C1 for isotopic analysis of $\delta^{13}C_{carb}$ and $\delta^{18}O$. Where possible, only articulated carapaces were picked to ensure that no transport or taphonomic alteration had occurred. Samples weighing between 200 and 300 μg were cleaned and sonicated in distilled water to remove any attached organic matter and then left to dry at room temperature for 24 hours. The samples were analyzed in an online carbonate system (ISOCARB) connected to a VG Optima isotope-ratio mass spectrometer at the McMaster University Stable Isotope Laboratory. The results were compared against NBS-19, with precision on replicate samples better than ±0.1‰. Results are presented here in standard delta notation in per mil (‰) against Vienna PeeDee Belemnite (VPDB).

Organic matter from C1 and C2 was sent to Beta Analytic Radiocarbon Dating Laboratory in Miami, Florida to constrain their ages. The radiocarbon age was calibrated against the IntCal04 database (Reimer et al. 2004) and presented in calendar years before present (cal yBP). Organic matter from cores C3 and C4 was sent to the NOSAMS laboratory at Woods Hole Oceanographic Institute in Massachusetts for radiocarbon dating. These dates were calibrated against the IntCal04 database using the freeware program CALIB (Stuiver and Reimer, 1993). An age-depth regression model was derived for C2 and C3 to allow for a more accurate correlation (Heegaard et al., 2005); an insufficient number of dates were obtained from C1 and C4 to allow for such a model.

Results

Lithology

The three cores that were obtained from the caves (C2, C3, and C4) were generally homogenous and consisted of organic gyttja, with total organic carbon ranging from 25 – 50%. Due to the high porosity and low density of the sediments, coring resulted in more than 50% compaction in all three cores; the core depths presented here are compacted values. Lighter and darker coloured horizons throughout the cores were indicative of the amount of carbonate material present. The only distinct change in lithology occurred in C3, which contained a horizon with large fragments (0.5 – 1mm) of gastropod shells (25 – 35cm). All three of these cores penetrated the sediment all the way to basal limestone of the cave passage.

The cenote core, C1, showed several changes in lithology. The upper portion of the core was almost entirely gastropod shells (>1mm) with a coarse sand matrix. At 23 cm there was a sharp transition to a dark, organic rich peat layer with no shell fragments (23 – 28 cm). From 28 cm to 35 cm there was another interval of concentrated gastropod shells in a coarse sand matrix, followed by fine-grained marl that continued from 35 cm to the bottom of the core at 45 cm. A limestone rock (~5 cm in diameter) from the collapse pile was found plugging the bottom of the core.

The sedimentation rates in C2 and C3 were very low and showed inverse trends. In C2 (closer to the cenote) the sedimentation rates were initially higher (~0.5 mm yr^{-1}) and 1 cm of sediment represented approximately 21 years of accumulation. This rate steadily declined through time and is currently only 0.15 mm yr^{-1}. C3 initially had very low sedimentation (~0.15 mm yr^{-1}) which increased steadily through time and is currently about 0.5 mm yr^{-1}. On average, 1 cm of compacted sediment in C2 represents approximately 48 years while 1 cm of compacted sediment in C3 represents 44 years. Since age models were not constructed for C1 and C4 their sedimentation rates represent an estimated value. The cenote (C1) had an average sedimentation rate of only 0.08 mm yr^{-1} since 3740 cal yBP and downstream in the cavern (C4) the sedimentation rate was 0.14 mm yr^{-1} since 3400 cal yBP.

Chronology

A total of 15 dates were obtained from the four cores to provide a chronology of sediment deposition in the system (Table 1). Most of the radiocarbon ages were in proper chronological order; however, there were two inversions observed. At the top of C3, the 2 - 3cm interval was dated to 1370 – 1295 cal yBP and the 21-22cm interval had a date of 530 – 430 cal yBP. As such, the date from the 2 – 3 cm interval was not included in the age-depth model of this core as it was likely contaminated by older organic matter (perhaps a large OM fragment). In C1, radiocarbon dates obtained from organic matter from 21 – 22 cm and 31 – 32 cm were 3370 – 3210 cal yBP and 3840 – 3630 cal yBP, respectively; however, a date obtained from a carbonate gastropod shell at 12cm was 4790 – 4520 cal yBP. This inversion is due to the hard-water effect of ^{14}C-deficient cave waters contaminating aquatic carbonate material, thus making it appear much older than it is; Hodell et al. (1995) observed a hard-water error of ~1200 years in Lake Chichancanab on the Yucatan Peninsula. Since there was virtually no terrestrial organic matter in this interval of C1, a hard-water effect could not be obtained for Yax Chen.

The chronology was derived by fitting a second-order polynomial to the depth-age data (Fig. 3). The top date of the core was assumed to be -50 years based on the datum of 1950 for radiocarbon dating methods (Arnold and Libby, 1949). The fitted line passes through the data points well with an r^2 value of 0.9881 and 0.9995 for C2 and C3, respectively. The second order polynomial was used to account for the differential compaction that resulted from the surface sediments undergoing less compaction than the basal sediments (Hodell et al., 2005).

Microfossils

A total of five thecamoebian and twelve foraminifer species were identified in the four cores following the taxonomy of Gabriel et al. (2009) and van Hengstum et al (2008; 2009). The downcore variations of the dominant species were plotted according to their relative fractional abundance (Fig. 4). The microfossil assemblage in all four cores was dominated by the euryhaline foraminifer *Ammonia tepida* (mean = 55.17%). These assemblages generally had good preservation indicating little taphonomic alteration due to dissolution. The cluster analysis of the cores did not prove to be effective as the intervals were found to be unconstrained. *Ammonia tepida* is highly cosmopolitan species and occupies a wide range of salinities (Hayward et al., 2004; Scott et al., 2001) and therefore may not be very useful to identifying changes in low salinity environments. Due to the dominance of *A. tepida* (> 50%) and relatively low abundances of most of the other species (< 10%) different data manipulations were used in an attempt to down-weigh the abundances of *A. tepida* (e.g. logarithmic transform, removal of *A. tepida*). Logarithmic transforms are typically used in biological studies with diverse populations that are heavily dominated by one species to scale down their significance (e.g. Rilov and Benayahu, 2000), but even this did not prove very effective. The poor effectiveness of the cluster analysis is likely the result of the low sedimentation rates. Since the cores were sampled at 1 cm intervals each sediment sample represents nearly 50 years of accumulation and so the populations will represent an average of the salinity shifts over that time period; this will be further evaluated in the discussion and has been examined in Gabriel et al., (submitted).

Based on the microfossil populations (composition and total concentration) and the stable isotope data the cores were divided into two biofacies (Fig. 4 & 5), using the trends in a few key taxa: medium-oligohaline (MO; <3.5 – 5 ppt) was defined by higher abundances of *Centropyxis* spp and *Ammonia tepida*, and high-oligohaline (HO; > 5 ppt), which was defined by higher abundances of *Elphidium* spp and other calcareous foraminifera like *Rosalina subaracuana* and *Physalidia simplex*. These classifications and identifying taxa follow van Hengstum et al (submitted) and van Hengstum et al. (2008).

The HO biofacies can be seen in the oldest sediments (> 3000 cal yBP) at the base of C1 (41 – 45 cm) and C2 (70 – 79 cm) and throughout C4. This is the only biofacies where *Physalidia simplex* (C1 and C2) and *Rosalina subaracuana* (C2) are present in significant abundances (mean 10% and 7%, respectively). These species are typically found in higher salinity environments such as lagoons and lower salt marshes (van Hengstum et al., submitted; van Hengstum et al. 2008, Javaux and Scott, 2003; Usera et al., 2002). In C1 there is a low abundance of thecamoebians (4%) however C2 shows an anomalously high abundance of *Centropyxis constricta* (12%).

The MO biofacies is found mainly in C2 and C3. In C2 it is represented in two intervals, 15 – 60 cm (3000 – 1000 cal yBP) and again from 0 – 7 cm (500 cal yBP – present). In C3, the MO biofacies is only found between 40 and 72 cm (3000 – 1000 cal yBP). This facies is characterized by the absence of lagoon foraminifera (*R. subaracuana*) and an overall increase in *A. tepida* (40% to 70%) and *Elphidium* spp. (11% to 20%). Spikes in the abundance of *Elphidium gunteri* are found at 32 – 33 cm (14%) and 50 – 51 cm (41%) in C2 and C3, respectively. Both of these intervals correspond to a date of 1700 – 1800 cal yBP. The MO is also seen in C1 (6 – 20 cm) and shows a similar spike in *E. gunteri* at 12 – 13 cm

(37%) therefore we assume that the age of this interval would be 1700 – 1800 cal yBP.

In contrast to the other cores C4 is located in a more saline environment due to its proximity to the coast and the thinning of the fresh-water lens, which is the reason that only the HO biofacies was found in this core. The core was entirely dominated by calcareous foraminifera with less than 5% of the population consisting of agglutinated foraminifera; no thecamoebian species were observed in this core. However, the spike in *E. gunteri* was evident in this core as well at 30 – 31 cm, which would imply an age between 1700 and 1800 cal yBP which fits the estimated sedimentation rate.

Organic Geochemistry

The strongest isotopic signals were observed in C2 and C3 (Fig. 4). The basal intervals of each core (75 – 80 cm and 80 – 100 cm, respectively) had $\delta^{13}C_{org}$ values around -27‰ and $\delta^{15}N$ values around 4.5‰. The TOC (~24%, C2; ~32%, C3) and TN (~2.5%, C2; ~1.5%, C3) were at their lowest levels and the C/N ratio was 14 and 18, respectively. Moving up core, there was a shift in the $\delta^{13}C_{org}$ to more negative values (-31‰ at the top of C2 and -32.5‰ at the top of C3), while the $\delta^{15}N$ showed an overall shift to more positive values from ~4.5‰ to ~7‰. Both cores showed a trend toward increasing TOC from the bottom up, with maximum values being observed around the middle of the core (45% at 35cm and 45.6% at 45cm, respectively), followed by an overall decrease to 32.8% and 26.7%, respectively, at the top. Since the TN is virtually unchanging in both cores, the C/N ratio generally followed the trend in TOC. Similar trends in the isotopic ratios can be seen in C4 (Fig. 5), although they were more constrained, with $\delta^{13}C_{org}$ values shifting from -27.6‰ at the base to -29.25‰ at the top and $\delta^{15}N$ values shifting from 4.5‰ to 6.2‰.

Discussion

Sedimentation patterns

There are three main types of sediment input into the caves: (1) organic matter that gets washed in through cenotes or percolates down through fissures/cracks in the limestone with meteoric rain water (Pohlman et al., 1997); (2) detrital calcite grains that get eroded out of the limestone; and (3) authigenic crystals that form calcite rafts at the water surface (Taylor and Chafetz, 2004). In the case of C2 and C3, the dominant source is organic matter washed in from the upstream cenotes creating a fine-grained gyttja. Overall, there is a lateral trend in sedimentation moving upstream from Yax Chen cenote. The onset of sedimentation occurred around 5000 cal yBP at the C3 site based on the age-depth regression analysis. Initially the rates were very low (0.12 mm yr^{-1}). Based on the geochemical data, the source of the sediments at this time is terrestrial. This can be seen in the more positive $\delta^{13}C_{org}$ values (~27‰), which are the same as the values for terrestrial organic matter (Pohlman et al., 1997), and the higher C/N ratio (~18). Sedimentation in the cenote likely started around the same time or even earlier, though no basal date is available in C1. The basal sediments in C1 are fine-grained silt and clay (marl). The top of the marl layer was dated to 3700 cal yBP so sedimentation in the cenote must have started prior to that period. The onset of sedimentation in C2 does not occur until ~3500 cal yBP. Initially, C2 has a relatively high rate of sedimentation (~0.5 mm yr^{-1}), which, in contrast to C3, gradually decreases through time. The modern sedimentation rate of C2 is 0.15 mm yr^{-1} while at C3 its 0.5 mm yr^{-1}.

The microfossil record begins around 4000 cal yBP in the cenote core and 3500 cal yBP in the cavern cores. This data matches well with that collected from Aktun Ha and the onset of cave sedimentation (Gabriel e al., 2009; van Hengstum et al., submitted). The main factor controlling the microfossil and hydrochemical fluctuations as documented in the cores (esp. C2 and 3) was likely mid-late Holocene climate change, specifically changing precipitation. Precipitation patterns have been well documented over the past 3500 years using oxygen isotopes and sulphur content in lake sediments from the Yucatan (e.g. Curtis et al., 1998; Hodell et al., 2001) and fluctuations in the titanium concentration in the anoxic sediments of the Cariaco Basin, Venezuela; increased titanium is the result of higher surface runoff due to increased precipitation (Haug et al., 2001; 2003; Fig. 4). In the Ox Bel Ha cores parallel changes in aquifer salinity were noted with more saline conditions corresponding with more arid periods as found in these other climate records. This is likely due to a decrease in turbulent mixing as a result of decreased hydrologic flow of the fresh water mass out to the coast (Moore et al., 1992; Stoessell, 1995). Periods with higher precipitation increase the flow velocity of the upper water mass, particularly at the coast, causing more mixing of the two water masses and more brackish conditions. It is likely that major storm events such as hurricanes would have an affect on the turbulent mixing as well (Beddows, 2004); however events of such short time spans would be nearly untraceable in the Yax Chen sediments due to the low sedimentation rate.

Coastal progradation as a result of sea-level stabilization during the mid-late Holocene is likely another factor affecting the discharge of water from the cave systems and turbulent mixing of the halocline. Increased sediment accumulation at the coastal margin is associated with an overall decrease in the hydrologic conductivity of the groundwater aquifer as it impedes discharge (Vacher, 1988; Vacher and Wallis, 1992). This would be expected to be more prominent with Holocene sea-level stabilization and coastal progradation.

Evolution of Ox Bel Ha

For the purposes of this discussion, the evolution of the cave system will be based on the two upstream cavern cores (C2 and C3), beginning at the time of microfossil colonization. These two cores have the most amounts of microfossil and geochemical data, as well as a very well defined chronology. Though the sediment record does not extend back far enough to identify the initial flooding of the cenote and cave system, which based on regional sea-level curves would have been around 7000 yBP (Toscano and MacIntyre, 2003), it does provide a record of salinity shifts as a result of hydrogeologic and climatic forcing through the late Holocene.

Phase 1: 3500 – 3000 Cal yBP

The precipitation was highly variable between 3500 and 3000 cal yBP though overall it was trending towards more arid conditions on the Yucatan Peninsula as a result of the southward movement of the ITCZ and increased variability in the El Niño Southern Oscillation (ENSO; Haug et al., 2001). There are microfossils that have colonized C2, nearest the cenote, by 3500 cal yBP however it is not until the end of this period that they colonized further upstream (C3). The fluctuations in precipitation (Haug et al., 2001) caused a heterogeneous mix of lagoonal (i.e more marine) foraminifera (*R. subaracuana)* and slightly brackish thecamoebians (*Centropyxis* spp.). This is to be expected due to the low sedimentation rates (1 cm of sediment represents about 27 years). The salinity through this time period would have to range between < 3.5 and 6 ppt in order for both these species to be present, based on their ecologic constraints (Javaux and Scott, 2003; van Hengstum et al., submitted). The highly variable environmental conditions result in unstable populations of microfossils and very low total concentrations (~1000 cc^{-1}).

Phase 2: 3000 – 1000 cal yBP

Though still highly variable, the precipitation begins to increase after 3000 cal yBP and stabilizes around 2500 cal yBP (Haug et al., 2001). The increased turbulence from the precipitation caused an increase in salinity to > 6 ppt. The assemblages in the upstream cores (C2 and C3) became more brackish, with an increase in *A. tepida* and agglutinated species of foraminifera (e.g. *S. lobata* and

T. macrescens) and a decrease in thecamoebians (*C. aculeata* and *C. constricta*). The downstream core (C4) still exhibits a marine assemblage, with calcareous foraminifera (*A.tepida* and *Elphidium* spp.) comprising more than 95% of the assemblage and a small population of agglutinated species making up the rest. In all four cores however, the total concentration of microfossils is increasing significantly, a trend that continues all the way through Phase 2, and indicates an overall stabilization of the system. The mechanism for this is likely two-fold: (1) Further progradation and coastal plugging decreasing the overall hydrologic flow; and (2) More stable precipitation allowing for more constant environmental conditions.

The geochemical data also support an increase of fresh meteoric water into the system due to higher precipitation. The higher C/N ratios observed in C2 and C3 (18 and 21, respectively) can be attributed to terrestrial input to the system (Mackie et al., 2005; Cloern et al., 2002). As there is very little surface runoff, the groundwater carries terrestrial organic matter through the vadose zone and into the cave waters through percolation. This is further supported by the $\delta^{15}N$ and $\delta^{13}C$ values, which are increasing indicating a shift towards a more dominant input of terrestrial organic matter

The precipitation is steadily declining by 2600 yBP. There is a significant drop in the C/N ratio towards the end of this phase from 2000 – 1000 yBP, particularly in C3 (down to 15), as well as a drop in $\delta^{13}C$ (C3; -30‰) indicating a stronger influence from aquatic plants and PPOM as a result of decreased surface runoff. This is coincident with a severe multi-year drought between 1300 and 1100 yBP, which was the driest period of the mid-late Holocene (Hodell et al., 1995, 2001) and is believed to be the cause of the Classic Period collapse of the Maya when many of the most prominent city centres were suddenly abandoned (Polk et al., 2007; Haug et al., 2003; Sharer, 1994).

Sedimentation rates are decreasing in C2 (0.25 mm yr^{-1}) however, rates in C3 are increasing (0.2 mm yr^{-1}) indicating that a lateral upstream shift of the sedimentation occurred as a result of the complete flooding of the cenote. This is attributed to decreased hydrologic flow rates causing the sediment to fall out of suspension closer to the nearest upstream cenote (van Hengstum et al., submitted). C3 is located approximately 200 m downstream of the cenote Tarpon I (see Fig 1B).

Phase 3: 1000 – 400 yBP

The start of Phase 3 coincides with the Post-Classic period of the Maya (Sharer, 1994) and the "Medieval Warm Period", where there is a brief return to wetter conditions, though overall the precipitation continues to decline. The Maya site of Tulum, located about 9 km north-northeast of cenote Yax Chen along the coast, was settled around 750 yBP. The central walled city likely had a population in the low hundreds but the surrounding region was probably between 1000-3000 inhabitants (Witschey, 2001). The data from Yax Chen show a distinct freshening period.

The microfossil assemblage shows a decrease in more saline species, such as *Elphidium* spp., and the euryhaline foraminifer *A.tepida*, with an increase in marsh/wetland species *S.lobata*, *T.macrescens*, and *M.fusca* (Barbosa et al., 2005) and thecamoebian species *Centropyxis*. The salinity is decreasing and approaching the ecological limits of centropyxids. By the end of the Medieval Warm Period (~700 cal yBP) the highest abundance of centropyxids can be seen (~40%) indicating that the salinity was < 3.5 ppt). High abundances of centropyxids are also seen in Aktun Ha during this period along with *Lagenodifflugia vas* and *Difflugia oblonga*. Again, due to its distance from the coast and greater thickness of the freshwater lens, Aktun Ha would be less saline then Yax Chen, which allows for the colonization of these fresher water thecamoebian species.

While understanding of Maya interaction with wetland resources is still in its infancy, studies have shown that the people were capable of not only working natural wetlands on the coastal plain, but planning and constructing their own canals and fields (e.g. Berry and McAnany, 2007; Beach et al., 2009). This increase in wetland area as a result of settlement and agricultural use by the Maya would likely contribute to the change in microfossil assemblage. Concomitantly, the freshening of groundwater aquifer in the region would have allowed for the successful agricultural productivity of the associated wetlands. Moreover, at this time a slight shift to more enriched values of $\delta^{13}C$ (~-27‰) is evident. Agricultural vegetation (C_4 metabolic pathway) is more enriched in ^{13}C and although typical values range between -16‰ and -9‰ (Polk et al., 2007; Mackie et al., 2005) it is likely that an increase in agricultural vegetation would cause a shift to more positive values of $\delta^{13}C$.

The trends in sedimentation rates continue through this period with decreasing sedimentation rates in the shallow upstream cave (C2; 0.16 mm yr^{-1}) and increasing rates further upstream in the cave (C3; 0.33 mm yr^{-1}). Sea-level rise has nearly stabilized and the level is very close to the modern level (<1 m difference; Toscano and MacIntyre, 2003), so the water level in the cenote is also likely very close to modern levels. As Phase 3 ends the "Little Ice Age" period begins, with a global change in atmospheric circulation causing a drop in temperature and precipitation in the northern hemisphere. This is evident in ice cores (e.g. Thompson et al., 1986; Kreutz et al., 1997) and pollen records (e.g. Chepstow-Lusty et al., 1998).

Phase 4: 400 yBP – present

The effects of the Little Ice Age (~500 – 100 yBP) caused dramatic cooling and a decrease in precipitation in the northern hemisphere (1 – 2°C; Kreutz et al., 1997). The sedimentary record from Cariaco Basin in Venezuela shows a strong decrease in riverine runoff indicative of a decline in precipitation (Haug et al., 2001). Although the precipitation is decreasing overall, it was highly variable through this time period (see Fig. 4). There is a decrease in the total concentration of microfossils in all four cores, which is likely due to the medial salinity (~6.3 ppt) of the modern cenote and the low sedimentation rates.

Ammonia tepida, the most cosmopolitan foraminifera species (Scott et al., 2001), still thrives and dominates the assemblage; however, the water is too saline for proper thecamoebian colonization and too fresh for colonization by other calcareous foraminifera (e.g. *Elphidium*). There is still a presence of agglutinated marsh foraminifera, which is not surprising due to the high organic content of the sediments. The presence of centropyxids in this phase shows that similar conditions of varying salinity were occurring as in Phase 1, resulting in a heterogeneous assemblage of microfossils

The geochemical data all suggest that the dominant input of organic matter into the system is from the cave waters, which is to be expected since surficial runoff is extremely low due to the high porosity of the limestone and the decreased precipitation. This period shows the most depleted values of δ^{13}C (~-31‰), which is close to the values presented by Pohlman et al. (1997) for the PPOM (-35‰). The 4‰ difference is likely caused by soil percolating down through the vadose zone, which was calculated to have a value of -25‰. This is supported by the δ^{15}N values of around 7.5‰, which are similar to the values that were measured for SPOM and cave benthic organic matter (CBOM). The decrease in C/N ratio to ~12 is indicative of dominant input from aquatic plants that are more nitrogen-rich (Müller and Voss, 1999; Cloern et al., 2002; Mackie et al., 2005)

The pattern of sedimentation in the upstream cave cores still continues. Sedimentation rate in C3 (further upstream) increased to 0.375 mm yr^{-1}, while the rate in C2 decreased to 0.125 mm yr^{-1}. This shows that during this period a significant flow remained almost all the way to the coast, but greatly diminished as the water exited the confined cave passage into the open cenote. The sedimentation rate in the downstream core (C4) had an average of 0.3 mm yr^{-1} since 1320 yBP, though without another date further upcore it is not possible to discern a sedimentation pattern between 400 yBP and the present.

Comparison to Aktun Ha evolution

The Aktun Ha cave system (~8.5 km inland) is the only other system on the Yucatan that has been studied with respect to its palaeoenvironmental record (van Hengstum et al., submitted). As with Ox Bel Ha, the sediment record in this system downstream from the one major cenote begins around 4200 years ago. In the Aktun Ha cave system (~8.5 km inland), decreased precipitation marks a shift in the microfossil assemblage from more saline (> 3.5 ppt) to fresher conditions (1.5 – 3.5 ppt) around 4200 cal yBP as a result of decreased turbulence of the mixing zone and more quiescent conditions (van Hengstum et al., submitted). Ox Bel Ha is closer to the coast where the thickness of the mixing zone is greater due to increased hydrologic shear between the outflowing fresh water lens and the inflowing marine water and tidal forcing (Moore et al., 1992; Beddows et al., 2007; Fig. 2). As such, it is understandable the salinity of Ox Bel Ha at this time is higher with more brackish foraminifera and thecamoebians and no presence of fresher water species such as *Difflugia*. These conditions can be seen in the modern systems as well, where the freshwater lens at Aktun Ha has a salinity of

~1.5 ppt and at Ox Bel Ha the surface waters are between 5 – 6 ppt. By 3300 cal yBP in Aktun Ha, sedimentation rates furthest downstream from the cenote are minimal when compared to the cave entrance close to the cenote (van Hengstum et al., submitted). As in Yax Chen, there is a lateral shift in the sedimentation patterns closer to the cenotes upstream. C3 is approximately 200 m downstream of cenote Tarpon 1 (see Fig. 1B) so sedimentation is trending upstream towards it as hydrologic conductivity downstream continues to decrease. This sedimentation trend continues through to modern times. In addition, the microfossils continue trending towards a fresh assemblage comprised of *Difflugia* spp. and *Lagenodifflugia vas* as a result of less turbulence at the mixing zone.

Implications for Maya archaeology

The effect of late Holocene climate change on the ancient Maya civilization has been the focus of several studies (e.g. Polk et al., 2007; Hodell et al., 2005; Haug et al., 2003; Curtis et al., 1998). Sedimentary records from inland lakes (e.g. Hodell et al., 2001) and caves (e.g. Polk et al., 2007) show strong correlations between severe long-term (~200 years; Hodell et al., 1995) drought periods and the collapse of the Classic Maya period around 1100 yBP. It is around this time however that major city-centres such as Chichen Itza, Mayapan, Tancah and Tulum started to rise along the coast (Sharer, 1994). It would appear that the end of the Classic Period is not so much of a collapse of the Maya civilization as it is a relocation of the prominent city-centres from the densely forested inlands to the coastal areas. Around 1200 yBP, there is a distinct freshening trend seen in the data from Ox Bel Ha, which indicates that through arid periods the cenotes and cave systems actually become fresher. This is a result of decreased turbulence and hydrologic flow due to less rainfall and increased coastal plugging from progradation. Consequently, the water column becomes more stratified during these quiescent times and fresher water is available at the surface. A similar pattern can be seen in Aktun Ha (~8 km west of Ox Bel Ha) where colonization of the cave by fresh water thecamoebian species *Difflugia oblonga* and *Lagenodifflugia vas* occurs around 2700 yBP as a result of decreased turbulent mixing of the groundwater (van Hengstum et al., in press).

Conclusions

The sedimentary record from the seaward edge of the Ox Bel Ha cave system shows four periods of environmental change over the past 4000 years. The dominant sediment input into the cave is organic matter originating from either the upstream cenote pools or terrestrial soil being carried through the vadose zone via meteoric water percolation. Changes in microfossil assemblages and organic geochemistry identify shifts in the salinity of the MW, which is closely linked to wider-scale climatic and environmental changes such as the movement of the ITCZ. An interesting relationship was observed which indicates that during more arid periods the cenote and cave water actually becomes fresher due to increased stratification of the water column. This has significant archaeological implications as it helps to understand the abandonment and repopulation of Maya cities, specifically between the Classic and Post-Classic Periods.

Our results indicate that the data from the sedimentary record within a coastal anchialine cave system are useful palaeoenvironmental indicators and they provide the only source of palaeoenvironmental change along the Caribbean coast at Holocene time scales. These results are part of a growing body of data from anchialine cave systems in the Yucatan that are helping to enhance our understanding of the response of this coastal karst aquifer to sea-level rise and climate change so we can better manage this valuable resource and plan for future change.

Acknowledgements

We gratefully acknowledge Francisco Hernandez Franco, Encargado de la Sémarnat (Quintana Roo); Gustavo Maldonado Saldaña, Director of Secretaria del Medio Ambiente y Ecología for the municipality of Solidaridad; Paul Sánchez-Navarro of Centro Ecológico Akumal; diving logistics and sampling from The Mexico Cave Exploration Project and Cindaq (F. Devos, C. Le Maillot, S. Meacham, and D. Riordan), and B. Wilson and E. Utigard for SCUBA support. Special thanks to F. Devos for drafting the cave map.

Funding was provided by The Royal Geographic Society (with The institute of British Geographers) Ralph Brown Expedition Award (EGR & PAB), National Geographic (Committee for Research and Exploration Grant; EGR & PAB), National Science and Engineering Research Council of Canada Post-Graduate Scholarship (PvH), and Discovery Grant (EGR); and Student Research Grants (to PvH) from: the Geological Society of America, the Cushman

Foundation for Foraminiferal Research, and the Sigma Xi Scientific Research Society.

References

Alcocer J, Lugo A, Marìn LE, Escobar E (1998) Hydrochemistry of waters from five cenotes and evaluation of their suitability for drinking-water supplies, northeastern Yucatan, Mexico. Hydrogeol J 6:293-301

Arnold JR, Libby WF (1949) Age Determinations by Radiocarbon Content: Checks with Samples of Known Age. Science 110:678-680

Back W, Hanshaw BB, Herman JS, Van Driel JN (1986) Differential dissolution of a Pleistocene reef in the ground-water mixing zone of coastal Yucatan, Mexico. Geology 14:137-140

Barbosa CF, Scott DB, Seoane JCS, Turcq BJ (2005) Foraminiferal zonations as base lines for Quaternary sea-level fluctuations in south-southeast Brazilian mangroves and marshes. J Foramin Res 35(1):22-43

Beach T, Luzzadder-Beach S, Dunning N, Jones J, Lohse J, Guderjan T, Bozarth S, Millspaugh S, Bhattacharya T (2009) A review of human and natural changes in Maya Lowland wetlands over the Holocene. Quaternary Sci Rev 28(17-18):1710-1724

Blanchon P, Shaw J (1995) Reef drowning during the last deglaciation: evidence for catastrophic sea level rise and ice sheet collapse. Geology 23:4-8

Blanchon P, Jones B, Ford DC (2002) Discovery of a submerged relic reef and shoreline off Grand Cayman: further support for an early Holocene jump in sea level. Sediment Geol 147:253-270

Brady JE (1997) Settlement Configuration and Cosmology: The Role of Caves at Dos Pilas. Am Anthropol 99(3):602-618

Chepstow-Lusty AJ, Bennett KD, Fjelds□ J, Kendall A, Galiano W, Herrera AT (1998) Tracing 4,000 Years of Environmental History in the Cuzco Area, Peru, from the Pollen Record. Mountain Research and Development 18(2):159-172

Cloern JE, Canuel EA, Harris D (2002) Stable carbon and nitrogen isotope composition of aquatic and terrestrial plants of the San Francisco Bay estuarine system. Limnol Oceanogr 47(3):713-729

Curtis JH, Hodell DA, Brenner M (1996) Climate variability on the Yucatan Peninsula (Mexico) during the past 3500 years, and implications for Maya cultural evolution. Quat Res 46:37-47

Curtis JH, Brenner M, Hodell DA, Balser RA, Islebe GA, Hooghiemstra H (1998) A multi-proxy study of Holocene environmental change in the Maya Lowlands of Peten, Guatemala. J Paleolimnol 19:139-159

Digerfeldt G, Hendry MD (1987) An 8000 year Holocene sea-level record from Jamaica: implications for interpretation of Caribbean reef and coastal history. Coral Reefs 5:165-169

Ellison J (1993) Mangrove retreat with rising sea-level, Bermuda. Estuar Coast Shelf Sci 37:75-87

Ellison RL, Nichols MM (1976) Modern and Holocene foraminifera in the Chesapeake Bay region. First international symposium on benthonic foraminifera of continental margins; Part A, Ecology and biology, Maritime Sediments:131-151

Fairbanks RG (1989) A 17,000 year glacio-eustatic sea level record; influence of glacial melting rates on the Younger Dryas even and deep ocean circulation. Nature 342:637-642

Freudenthal T, Wagner T, Wenzhöfer F, Zabel M, Wefer G (2001) Early diagenesis of organic matter from sediments of the subtropical Atlantic: evidence from stable nitrogen and carbon isotopes. Geochim Cosmochim Ac 65(11):1795-1808

Gabriel JJ, Reinhardt EG, Peros MC, Davidson DE, van Hengstum PJ, Beddows PA (2009) Palaeoenvironmental evolution of Cenote Aktun Ha (Carwash) on the Yucatan Peninsula, Mexico and its response to Holocene sea-level rise. J Paleolimnol 42(2):199-213

Gischler G, Hudson JH (2004) Holocene development of the Belize Barrier Reef. Sediment Geol 164:223-236

Hanshaw BB, Back W (1980) Chemical mass-wasting of the northern Yucatan Peninsula by groundwater dissolution. Geology 8:222-224

Haug GH, Hughen KA, Sigman DM, Peterson LC, Röhl U (2001) Southward Migration of the Intertropical Convergence Zone Through the Holocene. Science 293: 1304-1308

Haug GH, Günther D, Peterson LC, Sigman DM, Hughen KA, Aeschlimann B (2003) Climate and the Collapse of Maya Civilization. Science 299:1731-1735

Heegaard D, Birks HJB, Telford RJ (2005) Relationships between calibrated ages and depth in stratigraphical sequences: an estimation procedure by mixed-effect regression. The Holocene 15(4):612-618

Hodell DA, Curtis JH, Brenner M (1995) Possible role of climate in the collapse of Classic Maya civilization. Nature 375:391-394

Hodell DA, Brenner M, Curtis JH, Guilderson T (2001) Solar forcing of drought frequency in the Maya Lowlands. Science 292:1367-1370

Hodell DA, Brenner M, Curtis JH, Medina-Gonzalez R, Can EI, Albornaz-Pat A, Guilderson TP (2005) Climate change on the Yucatan Peninsula during the Little Ice Age. Quat Res 63:109-121

Horton BP, Culver SJ, Hardbattle MIJ, Larcombe P, Milne GA, Morigi C, Whittaker JE, Woodroffe SA (2007) Reconstructing Holocene Sea-Level Change for the Central Great Barrier Reef (Australia) Using Subtidal Foraminifera. J Foramin Res 37(4): 327-343

Iliffe TM (1992) An annotated list of the troglobitic anchialine fauna and freshwater fauna of Quintana Roo: *in* Navarro D, Suárez-Morales E (eds)

Diversidad Biologica en la Reserva de la Biosfera de Sian Ka'an Quintana Roo, Mexico, Volume 2: Centro de Investigaciones de Quintana Roo/Secretaria de Desarrollo Social, Chetumal, p. 197-215

Javaux EJ, Scott DB (2003) Illustration of Modern Benthic Foraminifera from Bermuda and Remarks on Distribution in Other Subtropical/tropical Areas. Palaeontol Electron 6(4): 29pp; http://palaeo-electronica.org/paleo/2003_1/benthic/issue1_03.htm

Johnston KJ (2004) Lowland Maya water management practices; the household exploitation of rural wells. Geoarchaeology 19(3):265-292

Kemp AC, Horton BP, Corbett DR, Culver SJ, Edwards RJ, van de Plassche O (2009) The relative utility of foraminifera and diatoms for reconstructing late Holocene sea-level change in North Carolina, USA. Quat Res 71:9-21

Kreutz KJ, Mayewski PA, Meeker LD, Twickler MS, Whitlow SI, Pittalwala II (1997) Bipolar changes in Atmospheric Circulation During the Little Ice Age. Science 277:1294-1296

Leyden BW (2002) Pollen evidence for climatic variability and cultural disturbance in the Maya Lowlands. Ancient Mesoamerica 13: 85-101

Loeblich AR, Tappan H (1998) Foraminiferal genera and their classification. Van Nostrand Reinhold Company Inc., New York

Lucero LJ (2002) The Collapse of the Classic Maya: A Case for the Role of Water Control. Am Anthropol 104(3):814-826

Mackie EAV, Leng MJ, Lloyd JM, Arrowsmith C (2005) Bulk organic ^{13}C and C/N ratios as palaeosalinity indicators within a Scottish isolation basin. J Quaternary Sci 20(4):303-312

Maddocks RF (2005) New thalassocypridine Ostracoda from anchialine caves of the Loyalty Islands, New Caledonia (Podocopida, Paracypridinae): Micropaleontology 51:169-216.

McCrary JK, Madsen H, González L, Luna I, López LJ (2008) Comparison of gastropod mollusc (Apogastropoda: Hydrobiidae) habitats in two crater lakes in Nicaragua. Rev Biol Trop 56(1):113-120

Medioli FS, Scott DB (1983) Holocene Arcellacea (Thecamoebians) from Eastern Canada: Cushman Found Spec Publ 21:5-63

Meyers PA (1994) Preservation of elemental and isotopic source identification of sedimentary organic matter. Chem Geol 114(3-4):289-302

Moore YH, Stoessell RK, Easley DH (1992) Fresh-water/sea-water relationship within a groundwater system, northeastern coast of the Yucatan Peninsula. Ground Water 30:343-350

Müller A, Voss M (1999) The palaeoenvironments of coastal lagoons in the southern Baltic Sea, II. ^{13}C and ^{15}N ratios of organic matter – sources and sediments. Palaeogeogr Palaeocl 145:17-32

Namiotko, T., Wouters, K., Danielopol, D. L., and Humphreys, W. F., 2004, On the origin and evolution of a new anchialine stygobitic Microceratina species (Crustacea, Ostracoda) from Christmas Island (Indian Ocean): J Micropalaeontol 23(1):49-59

Patterson RT, Fishbein E (1989) Re-examination of the statistical methods used to determine the number of point counts needed for micropaleontological quantitative research. J Paleontol 63(2):245-248

Patterson RT, Dalby A, Kumar A, Henderson LA, Boudreau EA (2002) Arcellaceans (thecamoebians) as indicators of land-use change: settlement history of the Swan Lake area, Ontario as a case study. J Paleolimnol 28:297-316

Patterson RT, Dalby AP, Roe HM, Guilbault JP, Hutchinson I, Clague JJ (2005) Relative utility of foraminifera, diatoms and macrophytes as high resolution indicators of paleo-sea level in coastal British Columbia, Canada. Quaternary Sci Rev 24:2002-2014

Phleger Jr. FB (1954) Some modern faunal and lithologic associations. J Sediment Petrol 24(2):135-136

Poag WC (1981) Ecologic Atlas of Benthic Foraminifera of the Gulf of Mexico: Marine Science International, Woods Hole, 174pp.

Pohlman JW, Iliffe TM, Cifuentes LA (1997) A stable isotope study of organic cycling and the ecology of an anchialine cave ecosystem. Mar Ecol Prog Ser 155: 17-27

Polk JS, van Beynen PE, Reeder PP (2007) Late Holocene environmental reconstruction using cave sediments from Belize. Quat Res 68:53-63

Quintana Roo Speleological Society (QRSS) (11 September 2009) List of long underwater caves in Quintana Roo, Mexico [Online]. Available: http://www.caves.org/project/qrss/qrlong.htm [Accessed online 28 Nov 2009]

Reimer PJ, Baillie MGL, Bard E, Bayliss A, Beck JW, Bertrand CJH, Blackwell PG, Buck CE, Burr GS, Cutler KB, Damon PE, Edwards RL, Fairbanks RG, Friedrich M, Guilderson TP, Hogg AG, Hughen KA, Kromer B, McCormac FG, Manning SW, Ramsey CB, Reimer RW, Remmele S, Southon JR, Stuiver M, Talamo S, Taylor FW, van der Plicht J, Weyhenmeyer CE (2004) IntCal04 terrestrial radiocarbon age calibration, 0-26 cal kyr BP. Radiocarbon 46: 1029-1058

Reinhardt EG, Little M, Donato S, Findlay D, Krueger A, Clark C, Boyce J (2005) Arcellacean (thecamoebian) evidence of land-use change and eutrophication in Frenchman's Bay, Pickering, Ontario. Environ Geol 47: 729-739

Rilov G, Benayahu Y (2000) Fish assemblage on natural versus vertical artificial reefs: the rehabilitation perspective. Mar Biol 136:931-942

Scott DB, Schafer CT, Medioli FS (1980) Eastern Canadian estuarine foraminifera: a framework for comparison. J Foramin Res 10(3):205-534

Scott DB, Hermelin JOR (1993) A device for precision splitting of micropaleontological samples in liquid suspension. J Paleontol 67: 151-154

Scott DB, Medioli FS, Schafer CT (2001) Monitoring in Coastal Environments Using Foraminifera and Thecamoebians: Cambridge University Press, Cambridge, UK. 172 pp.

Sharer RJ (1994) The Ancient Maya: Fifth Edition: Stanford University Press, Stanford, USA. 892pp.

Smart PL, Beddows PA, Coke J, Doerr S, Smith S, Whitaker FF (2006) Cave development on the Caribbean coast of the Yucatan Peninsula, Quintana Roo, Mexico. Geol Soc Am Spec Pap 404: 105-128

Stuiver M, Reimer PJ (1993) Extended 14C database and revised CALIB radiocarbon calibration program. Radiocarbon 35:215-230

Szabo BJ, Ward WC, Weidie AE, Brady MJ (1978) Age and magnitude of the late Pleistocene sea-level rise of the eastern Yucatan Peninsula. Geology 6:713-715

Thompson LG, Mosley-Thompson E, Dansgaard W, Grootes PM (1986) The Little Ice Age as Recorded in the Stratigraphy of the Tropical Quelccaya Ice Cap. Science 234:361-364

Toscano MA, Macintyre IG (2003) Corrected western Atlantic sea-level curve for the last 11,000 years based on calibrated ^{14}C dates from *Acropora palmata* framework and intertidal mangrove peat. Coral Reefs 22: 257-270

Turetsky MR, Manning SW, Wieder RK (2004) Dating Recent Peat Deposits. Wetlands 24(2):324-356

Vacher HL, Mylroie JE (2002) Eogenetic karst from the perspective of an equivalent porous medium. Carbonate Evaporite 17:182-196

van Hengstum PJ, Reinhardt EG, Beddows PA, Huang RJ, Gabriel JJ (2008) Thecamoebians (Testate Amoebae) and Foraminifera from three anchialine cenotes in Mexico: Low Salinity (1.5-4.5 psu) faunal transitions. J Foramin Res 38(4):305-317

van Hengstum PJ, Reinhardt EG, Beddows PA, Schwarcz HP, Gabriel JJ (2009) Foraminifera and testate amoebae (thecamoebians) in an anchialine cave: Surface distributions from Aktun Ha (Carwash) cave system, Mexico. Limnol Oceanogr 54(1):391-396

van Hengstum PJ, Reinhardt EG, Beddows PA, Gabriel JJ (in press) Investigating linkages between Holocene palaeoclimate and paleohydrogeology in Mexican anchialine cave sediments. Quaternary Sci Rev

Weidie AE (1985) Geology of the Yucatan Platform, in Ward WC, Weidie AE, Back W (eds.) Geology and Hydrogeology of the Yucatan and Quaternary Geology of the Northeastern Yucatan Peninsula, New Orleans Geological Survey Field Trip Guide, p. 1-19

Witschey WR (2001) Tulum, *in* Carrasco D (ed.) The Oxford Encyclopedia of Mesoamerican Cultures: The Civilizations of Mexico and Central America. Oxford University Press, New York, 1424pp.

Whitmore TJ, Brenner M, Curtis JH, Dahlin BH, Leyden BW (1996) Holocene climatic and human influences on lakes of the Yucatan Peninsula, Mexico:

An interdisciplinary, palaeolimnological approach. The Holocene 6: 273-287

Figure Captions

Figure 1: Study Area on the Yucatan Peninsula (A), the coastal extent of the Ox Bel Ha cave system (B) and the core locations (C). Note that this represents a small section of the Ox Bel Ha system. Map drafted by F. Devos

Figure 2: Hydrogeological model of mixing in the groundwater aquifer. The arrows represent flow direction. Cenote Aktun Ha has been the subject of a few recent studies involving palaeoenvironmental reconstructions and surface distributions of foraminifera and thecamoebians.

Figure 3. Age-depth regression analysis for C2 and C3. The error bars represent the 2 confidence interval of the ages. The age equation for C2: $age = -0.2168*d^2 + 61.681*d + 100.76$ ($r^2 = 0.9881$) and for C3: $age = 0.3197*d^2 + 18.843*d - 51.45$ ($r^2 = 0.9995$).

Figure 4. A: Northern and southern migration of the Intertropical Convergence Zone (ITCZ). B: Variations in precipitation based on titanium concentration in the anoxic sediments of the Cariaco Basin, Venezuela (adapted from Haug et al., 2001, 2003).

Figure 5. Downcore profiles of microfossils (foraminifera and thecamoebians) and organic geochemical proxies ^{13}C, ^{15}N, TOC, TN, and C/N) in C2 and C3. Depths were converted to ages using the respective age-depth equation. The biofacies are: HO – High Oligohaline, > 5 ppt; MO – Medium Oligohaline, < 3.5 – 5 ppt

Figure 6. Downcore profiles of microfossils (foraminifera and thecamoebians) and organic geochemical proxies ^{13}C, ^{15}N, TOC, TN, and C/N) in C1 and C4. Depths are presented in centimetres below sediment-water interface for these cores as there were not enough suitable dates for age-depth analysis. The biofacies are: HO – High Oligohaline, > 6 ppt; MO – Medium Oligohaline, < 3.5 – 6 ppt.

Tables

Table 1: Radiocarbon dates obtained from the four cores. Lab code Beta-XXXXXX are samples that were processed by Beta Analytic Laboratory and lab code OS-XXXXX are samples that were processed by the NOSAMS laboratory at the Woods Hole Oceanographic Institute. (*) denotes dates that were considered contaminated and excluded.

Core	Laboratory Code	Depth in core (cm)	Material Dated	Conventional Radiocarbon Age (^{14}C yBP)	$\delta^{13}C$ (VPDB)	Calendar Age 2σ confidence (cal yBP)
C1*	Beta-244013	12 – 13	Shell	4460 +/- 40	-2.1‰	4790 – 4520
C1	Beta-259712	21 – 22	Wood	3070 +/- 40	-27.5‰	3370 – 3210
C1	Beta-244014	31 – 32	Wood	3460 +/- 40	-26.6‰	3840 – 3630
C2	Beta-257280	9 – 10	Gyttja	950 +/- 40	-27.6‰	940 – 780
C2	Beta-257281	29 – 30	Gyttja	1840 +/- 40	-28.7‰	1870 – 1700
C2	Beta-257282	51 – 52	Gyttja	2460 +/- 40	-27.8‰	2720 – 2360
C2	OS-74418	73 – 75	Gyttja	3310 +/- 30	-27.6‰	3620 – 3470
C3*	OS-74419	2 – 3	Gyttja	1430 +/- 25	-30.0‰	1370 – 1295
C3	OS-74462	21 – 22	Gyttja	435 +/- 35	-27.9‰	534 – 437
C3	OS-74420	41 – 42	Gyttja	1410 +/- 30	-29.9‰	1360 – 1285
C3	OS-74422	61 – 62	Gyttja	2270 +/- 25	-29.0‰	2350 – 2180
C3	OS-74423	69 – 70	Gyttja	2730 +/- 25	-30.2‰	2870 – 2770
C3	OS-74424	79 – 80	Gyttja	3240 +/- 30	-27.6‰	3560 – 3390
C4	OS-74425	34 – 35	Gyttja	1390 +/- 30	-26.8‰	1350 – 1280
C4	OS-74426	42 – 43	Gyttja	3160 +/- 30	-27.5‰	3450 – 3340

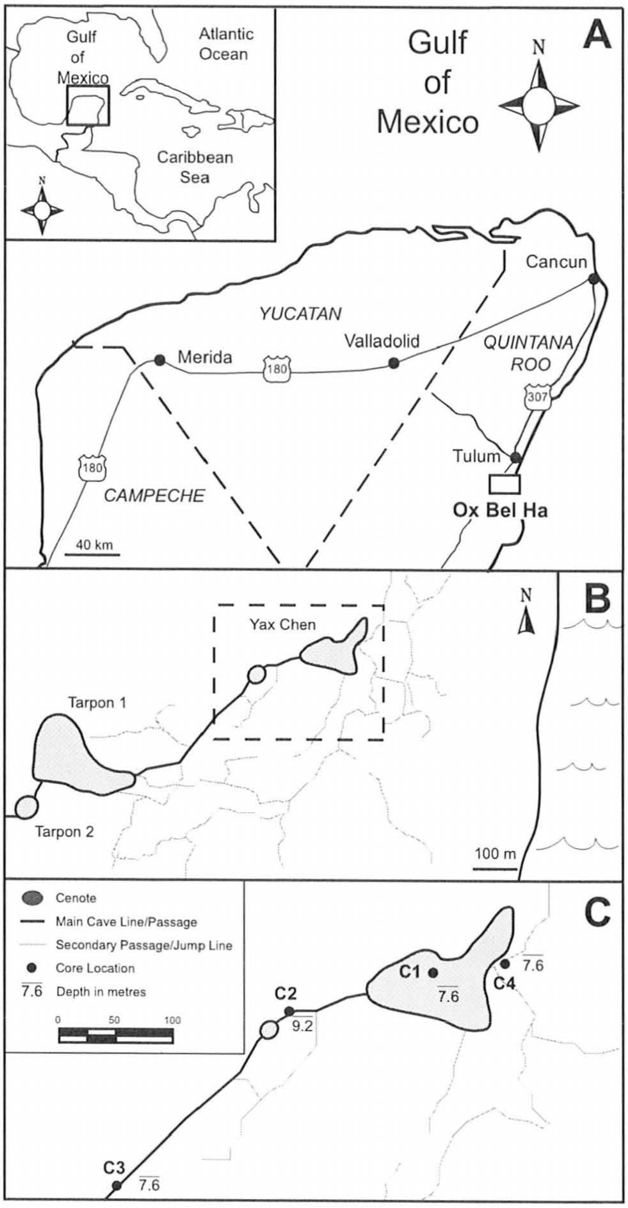
A
Gulf of Mexico
Atlantic Ocean
Caribbean Sea
N
Gulf of Mexico
Cancun
YUCATAN
Valladolid
Merida
180
QUINTANA ROO
307
Tulum
180
CAMPECHE
Ox Bel Ha
40 km
B
N
Yax Chen
Tarpon 1
Tarpon 2
100 m
C
Cenote
Main Cave Line/Passage
Secondary Passage/Jump Line
Core Location
7.6 Depth in metres
0
50
100
C1
7.6
C4
7.6
C2
9.2
C3
7.6

Figure 1

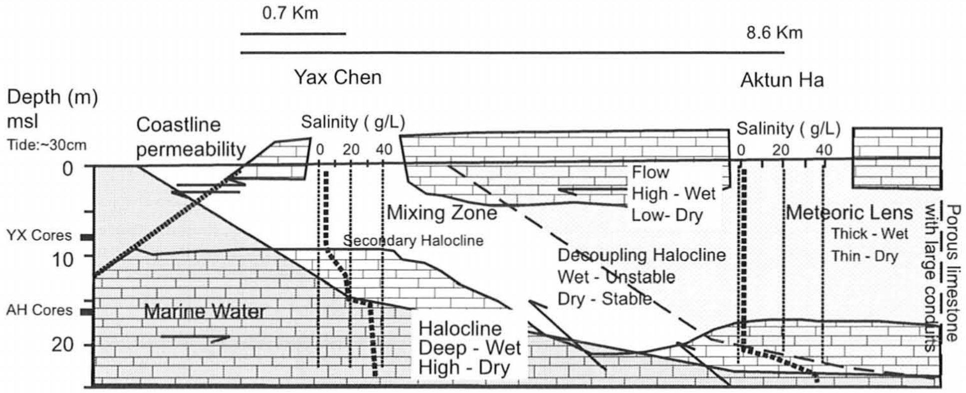
0.7 Km
8.6 Km
Yax Chen
Aktun Ha
Depth (m)
msl
Tide:~30cm
0
YX Cores
10
AH Cores
20
Coastline
permeability
Salinity (g/L)
0 20 40
Salinity (g/L)
0 20 40
Flow
High - Wet
Low- Dry
Mixing Zone
Meteoric Lens
Thick - Wet
Thin - Dry
Secondary Halocline
Decoupling Halocline
Wet - Unstable
Dry - Stable
Marine Water
Halocline
Deep - Wet
High - Dry
Porous limestone
with large conduits

Figure 2

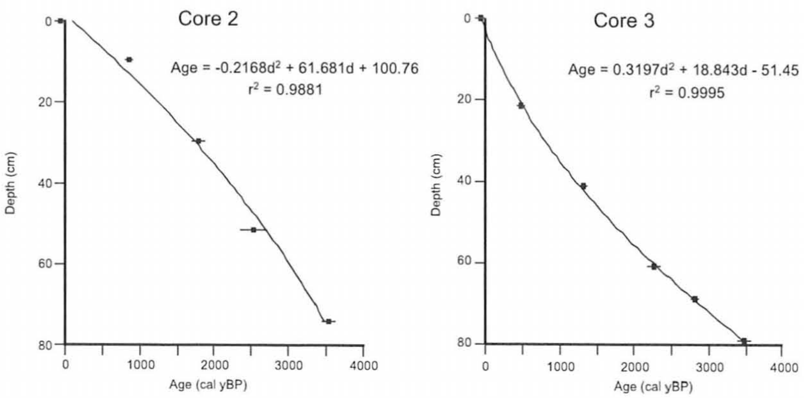
Core 2
Age = -0.2168d^2 + 61.681d + 100.76
r^2 = 0.9881
Depth (cm)
0
20
40
60
80
0
1000
2000
3000
4000
Age (cal yBP)
Core 3
Age = 0.3197d^2 + 18.843d - 51.45
r^2 = 0.9995
Depth (cm)
0
20
40
60
80
0
1000
2000
3000
4000
Age (cal yBP)

Figure 3

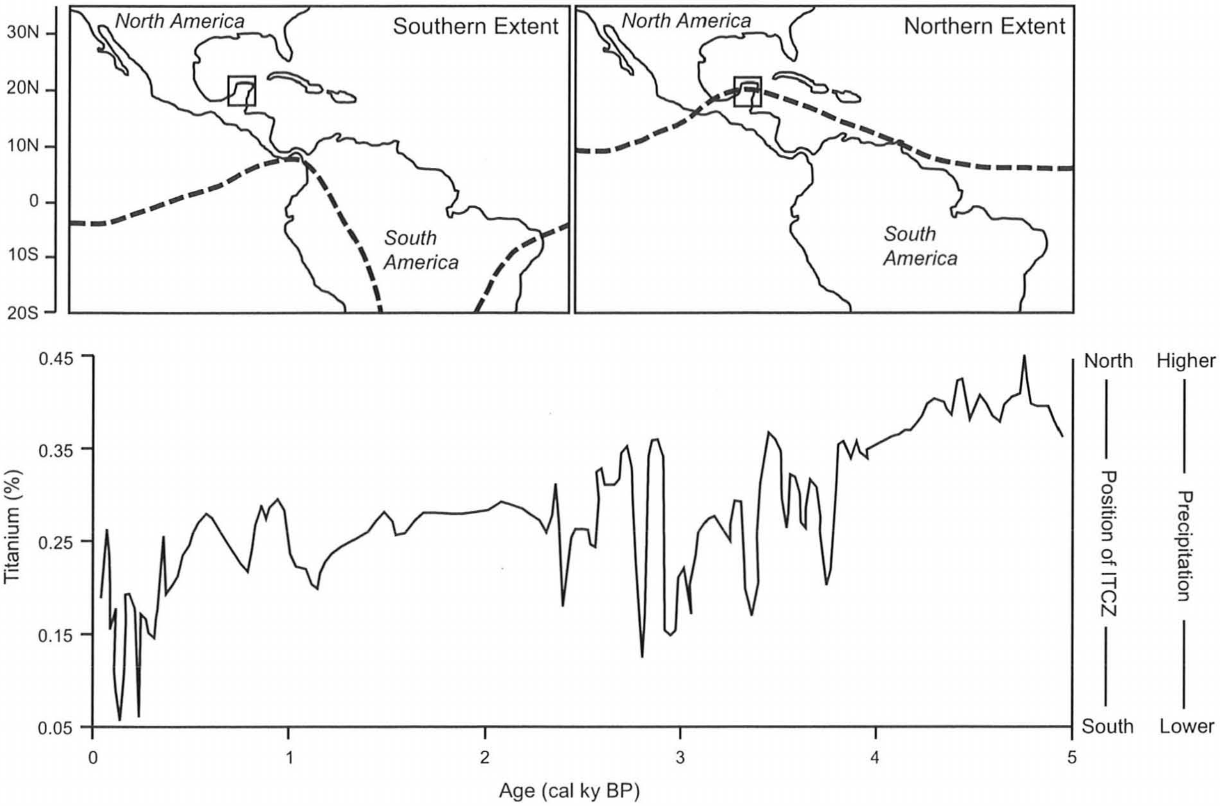
North America
Southern Extent
South America
North America
Northern Extent
South America
30N
20N
10N
0
10S
20S
Titanium (%)
0.45
0.35
0.25
0.15
0.05
0
1
2
3
4
5
Age (cal ky BP)
North
South
Position of ITCZ
Higher
Lower
Precipitation

Figure 4

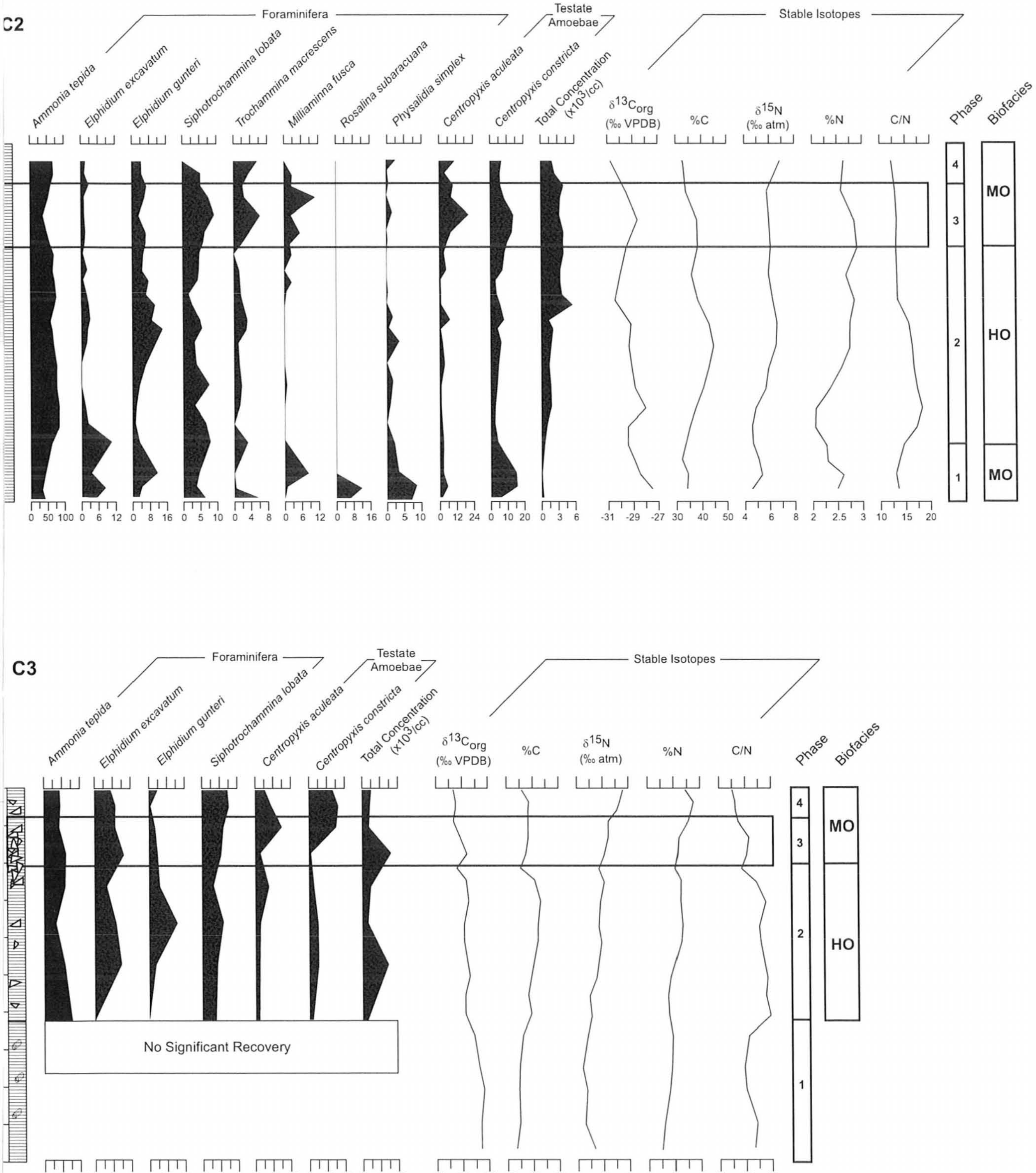
C2
Foraminifera
Testate Amoebae
Stable Isotopes
Ammonia tepida
Elphidium excavatum
Elphidium gunteri
Siphotrochammina lobata
Trochammina macrescens
Milliaminna fusca
Rosalina subaracuana
Physalidia simplex
Centropyxis aculeata
Centropyxis constricta
Total Concentration ($x10^3$/cc)
$\delta^{13}C_{org}$ (‰ VPDB)
%C
$\delta^{15}N$ (‰ atm)
%N
C/N
Phase
Biofacies
4
3
2
1
MO
HO
MO
0 50 100
0 6 12
0 8 16
0 5 10
0 4 8
0 6 12
0 8 16
0 5 10
0 12 24
0 10 20
0 3 6
-31 -29 -27
30 40 50
4 6 8
2 2.5 3
10 15 20
C3
Foraminifera
Testate Amoebae
Stable Isotopes
Ammonia tepida
Elphidium excavatum
Elphidium gunteri
Siphotrochammina lobata
Centropyxis aculeata
Centropyxis constricta
Total Concentration ($x10^3$/cc)
$\delta^{13}C_{org}$ (‰ VPDB)
%C
$\delta^{15}N$ (‰ atm)
%N
C/N
Phase
Biofacies
4
3
2
1
MO
HO
No Significant Recovery
0 50 100
0 4 8
0 25 50
0 3 6
0 5 10
0 12 24
0 5 10
-34 -30 -26
20 40 60
4 6 8
1 2 3
10 16 22

Figure 5

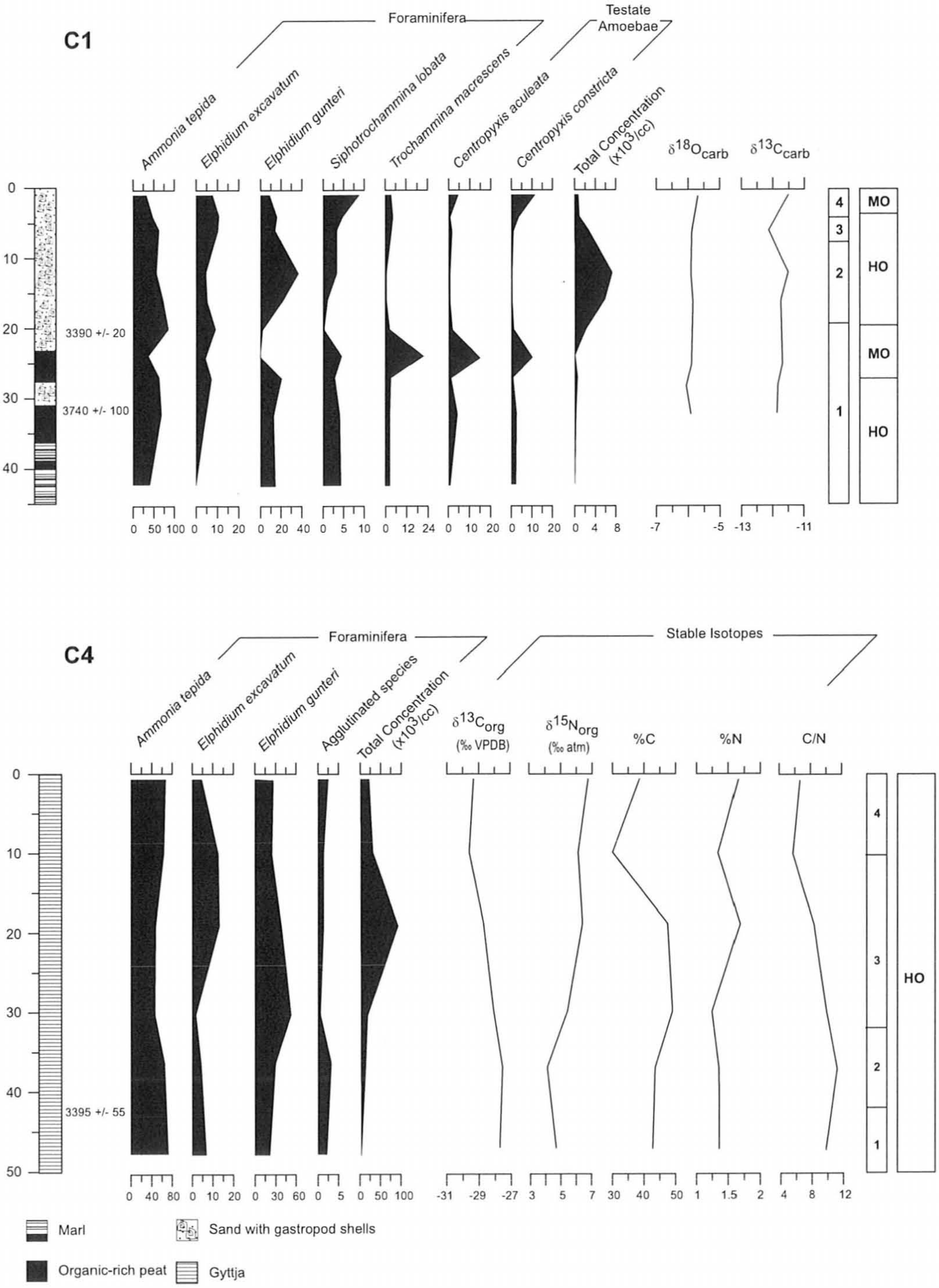
C1
Foraminifera
Testate Amoebae
Ammonia tepida
Elphidium excavatum
Elphidium gunteri
Siphotrochammina lobata
Trochammina macrescens
Centropyxis aculeata
Centropyxis constricta
Total Concentration (x10³/cc)
δ18Ocarb
δ13Ccarb
0
10
20
30
40
3390 +/- 20
3740 +/- 100
4
3
2
1
MO
HO
MO
HO
0 50 100
0 10 20
0 20 40
0 5 10
0 12 24
0 10 20
0 10 20
0 4 8
-7 -5
-13 -11
C4
Foraminifera
Stable Isotopes
Ammonia tepida
Elphidium excavatum
Elphidium gunteri
Agglutinated species
Total Concentration (x10³/cc)
δ13Corg (‰ VPDB)
δ15Norg (‰ atm)
%C
%N
C/N
0
10
20
30
40
50
3395 +/- 55
4
3
2
1
HO
0 40 80
0 10 20
0 30 60
0 5
0 50 100
-31 -29 -27
3 5 7
30 40 50
1 1.5 2
4 8 12
Marl
Sand with gastropod shells
Organic-rich peat
Gyttja

Figure 6

Chapter 4 – Conclusion

The anchialine cave systems of the Yucatan Peninsula represent a unique, low-salinity environment. Climate change through the mid-late Holocene has had a significant impact on the environmental conditions of Ox Bel Ha, primarily due to variations in precipitation patterns.

The modern distribution of foraminifera and thecamoebians in Ox Bel Ha proved to be responding to environmental conditions in a similar way to other cenotes and cave systems on the Yucatan Peninsula. However, sedimentation rates were a significant factor controlling sample biasing through time averaging. On average, 1 cm of sediment represented 50 years in the main conduit and near the cenotes. Those samples that were collected in the main conduit close to open cenotes had higher sedimentation rates and thus assemblages that more accurately described the modern conditions. The samples that were collected from deep in the cave where sedimentation rates are extremely low and salinity is higher (~12 ppt) had heterogeneous assemblages comprised of calcareous marine foraminifera like *Elphidium* spp. and freshwater thecamoebians (*Centropyxis* spp.) indicating that these samples were documenting several salinity shifts, likely over a few hundred years. When conducting further research in this environment (i.e. other anchialine cave systems, particularly on the Yucatan), samples should be only collected from areas with significant sedimentation; the amount of sediment in an area can be easily determined by probing. The results here demonstrate that in extremely low sedimentation environments the taphocoenosis dominates the assemblage over the biocoenosis. Isolating the living species via biological stain (e.g. Rose Bengal) will be much more effective at describing the modern environmental conditions.

The sedimentary record proved to be useful at reconstructing mid-late Holocene environmental changes as a result of climatic variations. An interesting relationship was evident in the microfossil and organic geochemical data, which showed that periods of decreased precipitation (drought) led to a concomitant decrease in salinity. The mechanism for this relationship is that during periods of lower precipitation the hydrologic conductivity of the superior meteoric water lens was decreased, which results in less turbulent mixing at the halocline. Once again, sample bias from poor time averaging as a result of low sedimentation must be taken into consideration. During times of high fluctuations in precipitation the assemblages are more heterogeneous and contain both foraminifera and thecamoebians, indicating salinity ranges of < 3.5 ppt and 6 ppt; more stable conditions result in more homogeneous assemblages. Correlations can be seen between fresher periods in Yax Chen and the start of the Post-Classic Period of the Maya when several coastal towns came into prominence. It would appear that as drought conditions persisted on the interior of the peninsula as a result of lower rainfall, the coastal cenotes became fresher due to the decreased hydrologic conductivity and less turbulent mixing of the fresh and saline groundwater.

These results are part of a growing body of research that aims to describe the current and palaeo-hydrologic conditions in low-salinity, anchialine caves on the Yucatan. This data will help in monitoring and management of the groundwater aquifer on the Yucatan in response to increased anthropogenic pressures, near-future climate change, and rising sea levels.